

Photogrammetric Techniques for Evaluation and Analysis of Concrete Structures and Specimens

Nicolas D'Amico

Graduate Masters Thesis
Advisor: Tzuyang Yu
Department of Civil and Environmental Engineering
The University of Massachusetts Lowell
Lowell, Massachusetts

SERG

Outline

- **Introduction**
- **Objective**
- **Photogrammetry**
- **Other Approaches**
- **Methodology**
- **Lab Specimen Results**
- **In-Situ Test Results**
- **Summary and Conclusion**
- **Contributions**
- **Acknowledgements**
- **References**

Introduction

- **Civil Infrastructure Deterioration**

- As Civil engineers across America struggle to push back the dividend of a necessary investment, new techniques need to be brought to light and old ones need to be reformed.

- **D: “POOR: AT RISK**

Category	1988*	1998	2001	2005	2009	2013
Aviation	B-	C-	D	D+	D	D
Bridges	-	C-	C	C	C	C+
Dams	-	D	D	D+	D	D
Drinking Water	B-	D	D	D-	D-	D
Energy	-	-	D+	D	D+	D+
Hazardous Waste	D	D-	D+	D	D	D
Inland Waterways	B-	-	D+	D-	D-	D-
Levees	-	-	-	-	D-	D-
Public Parks and Recreation	-	-	-	C-	C-	C-
Rail	-	-	-	C-	C-	C+
Roads	C+	D-	D+	D	D-	D
Schools	D	F	D-	D	D	D
Solid Waste	C-	C-	C+	C+	C+	B-
Transit	C-	C-	C-	D+	D	D
Wastewater	C	D+	D	D-	D-	D
Ports	-	-	-	-	-	C
America's Infrastructure GPA	C	D	D+	D	D	D+
Cost to Improve	-	-	\$1.3 trillion	\$1.6 trillion	\$2.2 trillion	\$3.6 trillion

**The first infrastructure grades were given by the National Council on Public Works Improvements in its report Fragile Foundations: A Report on America's Public Works, released in February 1988. ASCE's first Report Card for America's Infrastructure was issued a decade later.*

(Source: ASCE 2013 infrastructure report card.)

Introduction

■ Civil Infrastructure Deterioration

- On April 8, 2015 the MBTA submitted an action plan which called for the transformation of the MBTA due to what they describe as “pervasive structural failures”

“Some have called the winter of 2015 a ‘stress-test’ for the MBTA. While the MBTA ‘survived’ the test, short-term costs were significant in disruption, economic losses, and public and private hardship. The long-term costs are even more troubling: the loss of public confidence in our regional transit system.” (MBTA panel report)

**MBTA
Reported:**

Asset Category	# of Assets	Replacement Value	SGR Score	SGR Backlog Amount	% of Total Backlog
Revenue Vehicles	20,262	\$6,807,342,488	2.83	\$2,634,418,286	39.4%
Bridges	1,335	\$5,148,275,301	3.39	\$799,663,040	11.9%
Signals	401	\$2,900,740,296	2.57	\$1,369,027,122	20.5%
Stations	50,054	\$2,699,874,652	3.86	\$255,984,809	3.8%
Facilities	2,855	\$1,527,289,845	3.19	\$477,930,928	7.1%
Track/ROW	129	\$823,254,368	2.69	\$304,603,884	4.6%
Power	3,047	\$793,073,100	2.18	\$462,319,775	6.9%
Parking	47,215	\$228,188,855	2.12	\$172,050,515	2.6%
Communications	15,334	\$172,916,740	4.25	\$3,195,090	0.0%
Technology	1,092	\$138,231,180	1.39	\$131,592,980	2.0%
Tunnels	67	\$132,750,000	3.10	\$24,000,000	0.4%
Non-Revenue Vehicles	1,089	\$77,414,330	2.70	\$33,724,000	0.5%
Fare Collection	2,982	\$64,152,548	3.79	\$425,000	0.0%
Elevators and Escalators	338	\$49,370,000	2.94	\$22,950,000	0.3%
	146,200	\$21,562,873,703	3.05	\$6,691,885,429	100%

Source: MBTA

(Source: MBTA Panel Report)

Introduction

- **Civil Infrastructure Deterioration**
 - On July 10th, 2015 a piece of debris fell from the Commonwealth Ave. in Boston down to Mass Ave below
 - Anderson bridge in Harvard restoration costs the state millions



(Source: The Boston Herald (photo by Chitose Suzuki))



(Source: The Boston Globe (photo by Daniel Ryan))

Introduction

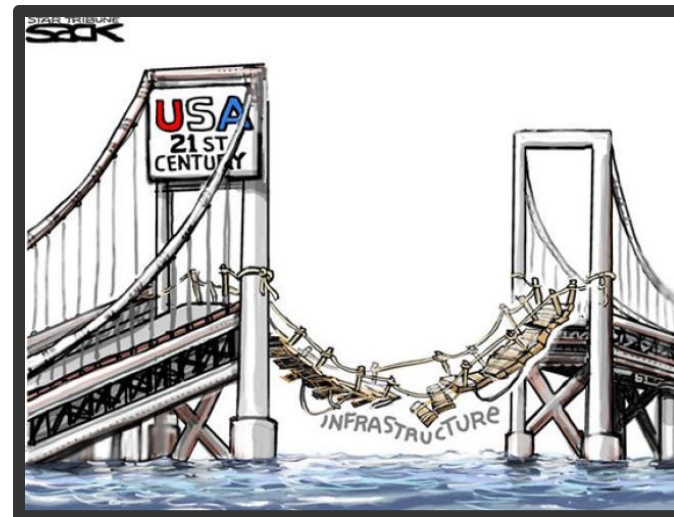
■ Civil Infrastructure Deterioration

- “Most of our road, rail, water, sewer, electric power, wired telephone, and other distributed systems infrastructure are old and in need of repair. Our ports, airports, and rail terminals are archaic, ill designed, badly run, and *poorly maintained*. Levees, coastal defenses, and dams often **lack effective inspection and maintenance**”

(Ernst G. Frankel, America's Infrastructure Dilemma, M.I.T Faculty newsletter, Vol. XX No. 1 September/October 2007)



(Source: Sustainable Cities Collective, website)



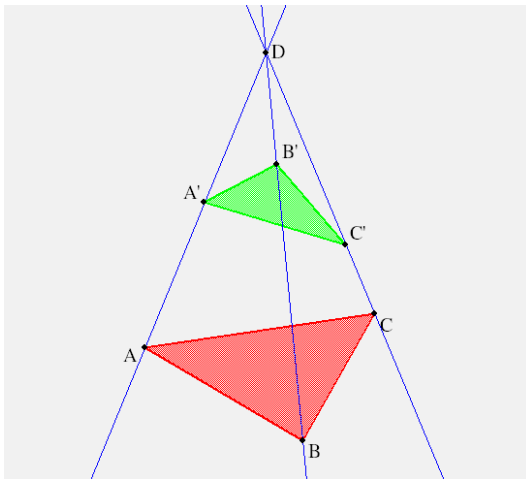
(Source: Steve Sack politic Cartoonist Star Tribune)

Objective

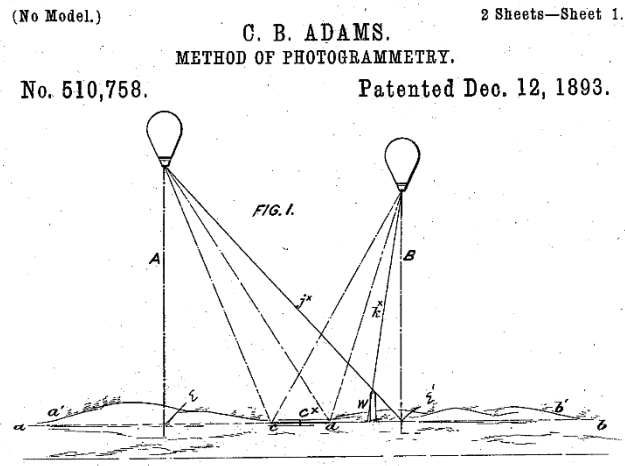
- To investigate how photogrammetry can be used to create geometrically accurate point cloud models PCM which can be used on laboratory specimens as well as in-situ structures. Furthermore, how PCM can be used for visual inspection as well as data integration of Synthetic aperture radar (SAR), rebound hammer (RBH), and digital image correlation (DIC) results. As well as how photogrammetric PCM can be used to conduct condition assessment including geometric analysis, surface crack profiling, mechanical loading analysis and even finite element modeling (FEM).

Photogrammetry

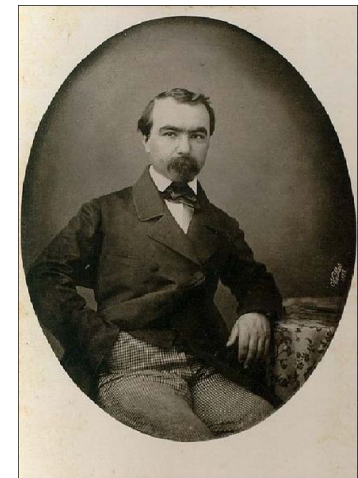
- (1648) Girard Desargues opens the scientific field of projective geometry with his theorem Desargue's Theorem which identifies a center of perspective and axis of perspectivity.



(Source: <http://new.math.uiuc.edu/>)



(Source: PBS GIS)



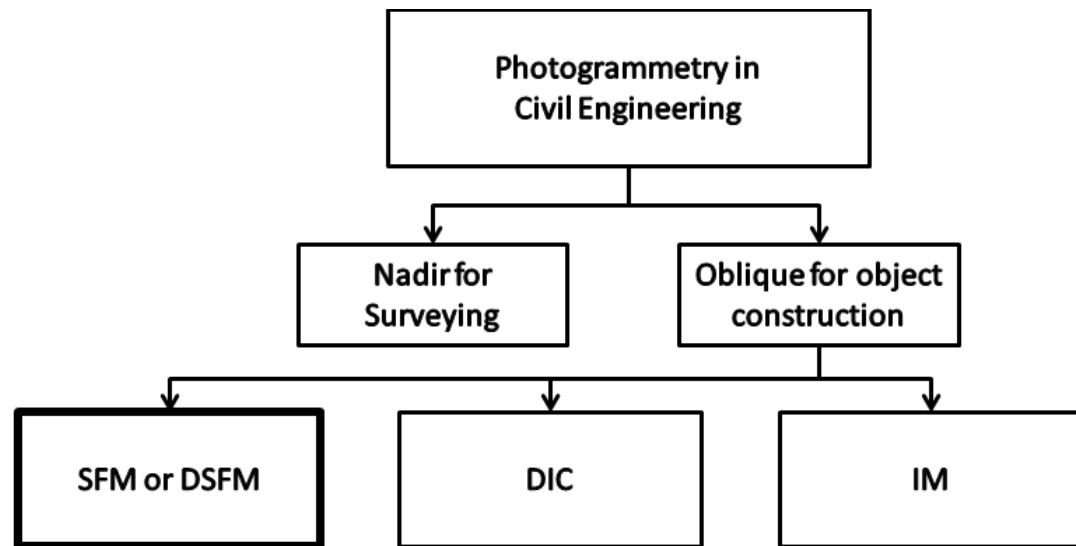
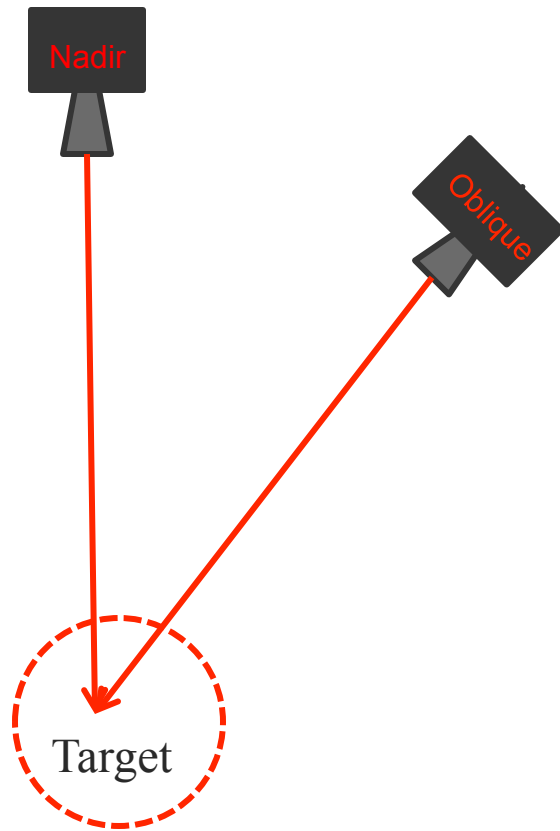
(Source: Wiki- public images)

- (1849) Aime` Laussedat develops Metrophotography, which is photographic surveying for maps. Coined as the father of photogrammetry

Photogrammetry

- **Image Capturing**

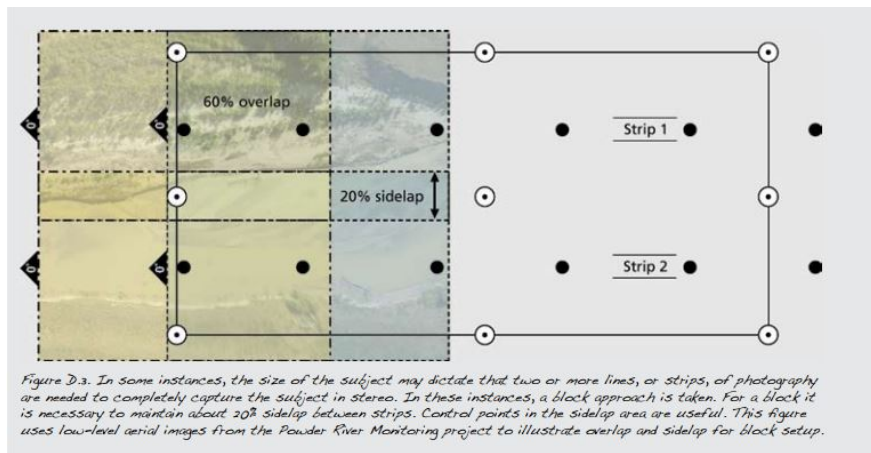
- Image collection techniques are broken into two key sub-categories.
- **Nadir** and **Oblique** Photogrammetry



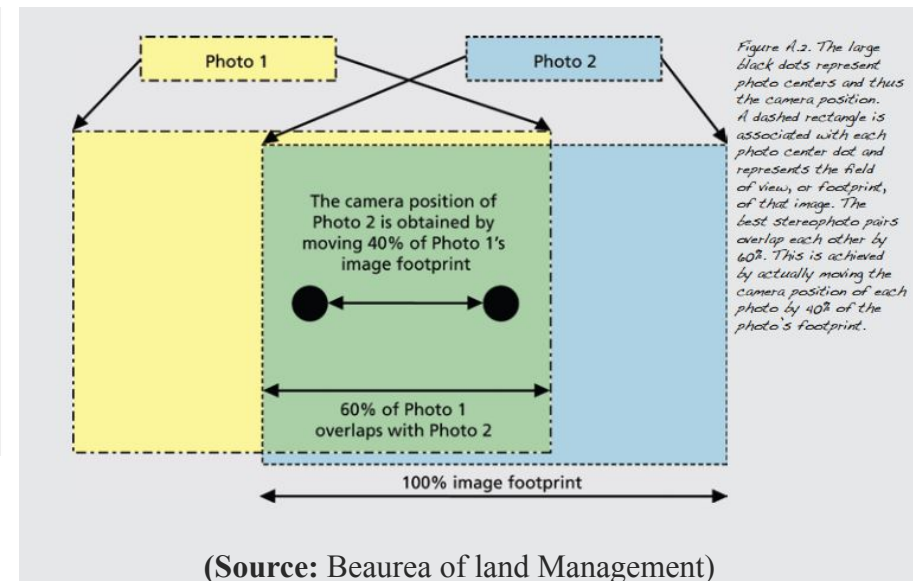
Photogrammetry

■ Image Capturing

- **Nadir- Aerial** is image taking from directly above (90°) the Point of interest
- This approach is meant for aerial mapping of large areas rather than singular structures, and is thereby effective for imaging of large masses of land.
- Most of the current UAV Photogrammetry is in this fashion



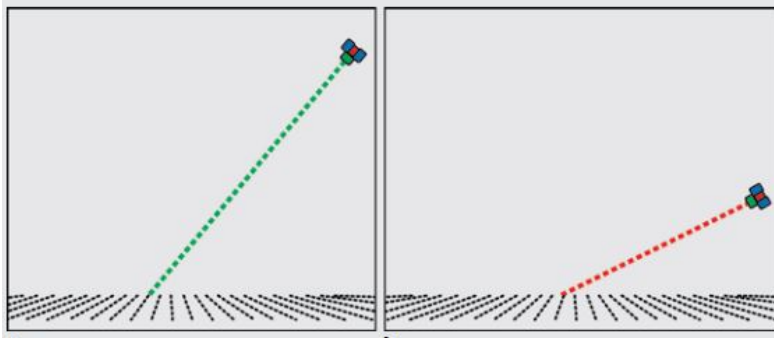
(Source: Beaura of land Management)



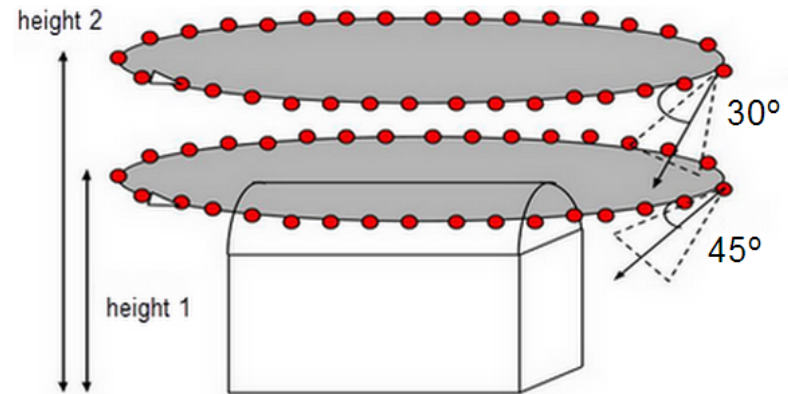
Photogrammetry

■ Image Capturing

- **Oblique Targeting** is image capturing aimed (obliquely) at one structure and uses multiple image perspectives and angles to triangulate and calculate dimensions.
- If the oblique angle is too acute the image is lacking a lot of spatial recognition. Between 30° - 90° is recommended.



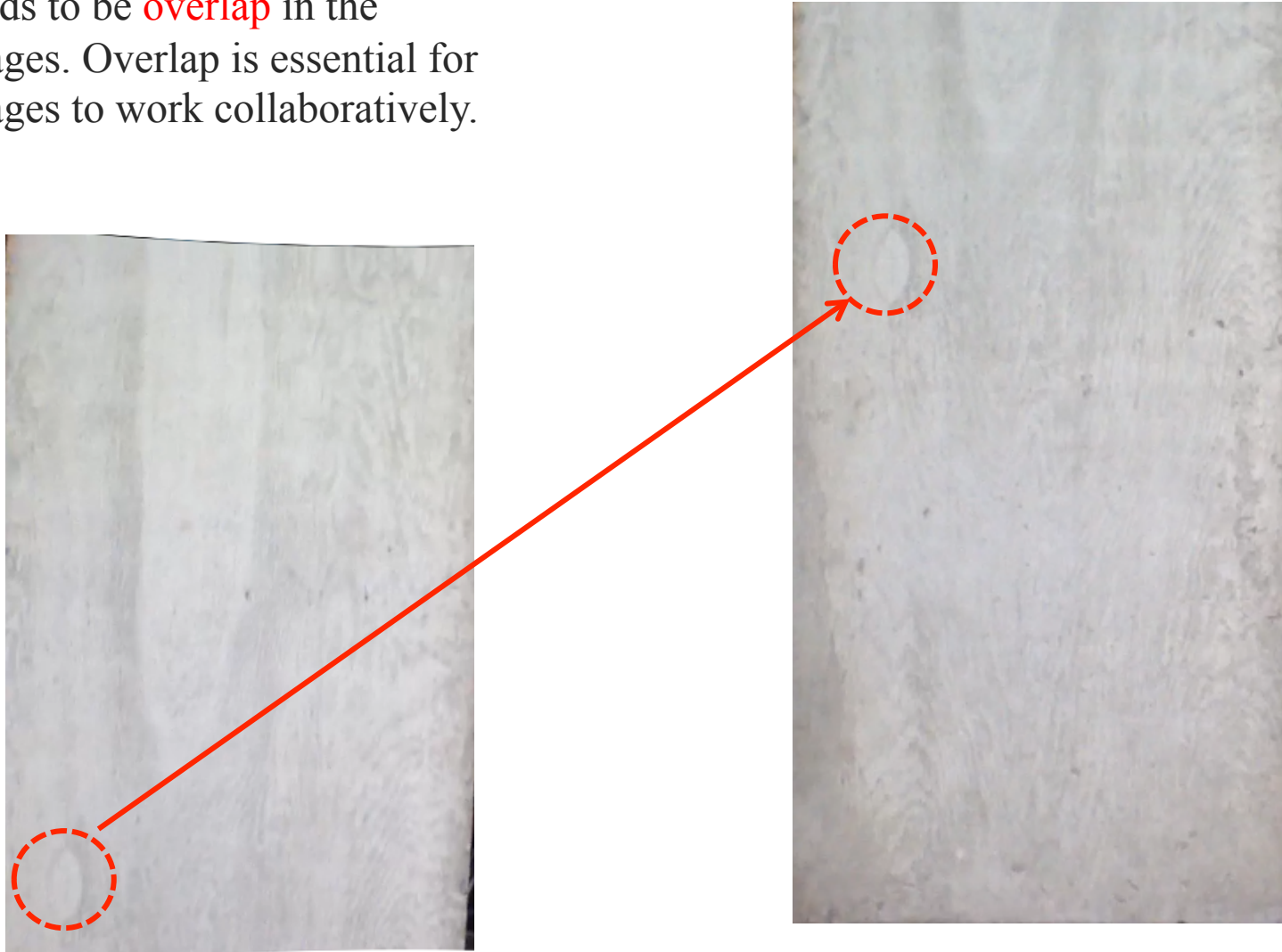
(Source: Beaura of land Management)



(Source: Pix4d support website)

Photogrammetry

- Photogrammetry uses **key points** to match images to start creating the models. This means that their needs to be **overlap** in the images. Overlap is essential for images to work collaboratively.



Photogrammetry

- **Depth** is the in or out of plane distances in a 2D image. Or the imaginary **third dimension** in a flat picture
- In a single 2D image depth perception is a non quantifiable illusion. It is however possible to use multiple perspectives to create **a stereo depth perception.**
- By locating all of the differences between two identical points in an image it is possible to start location 3D information which in turn helps create a 3D image.

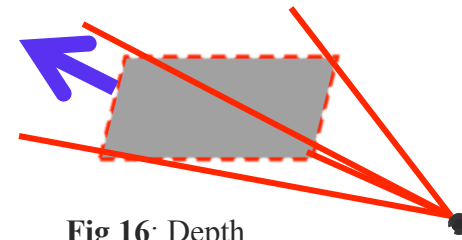


Fig 16: Depth

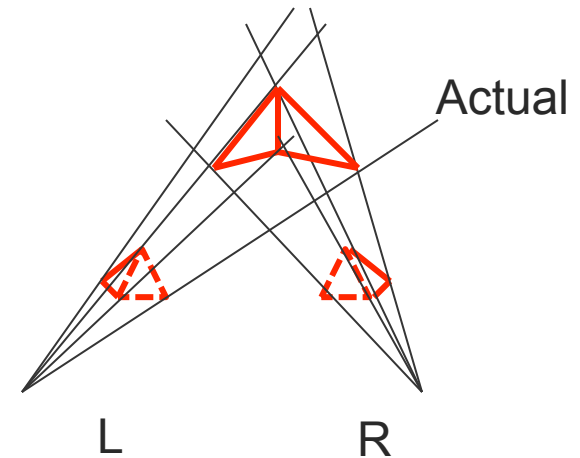
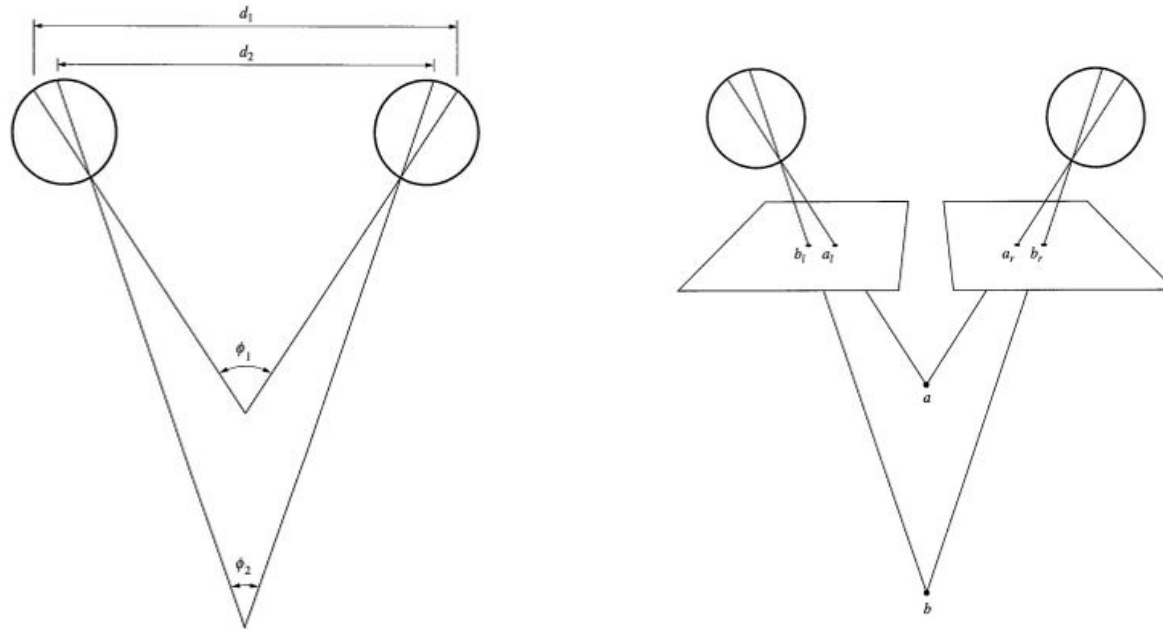


Fig 17: Stereo Depth

Photogrammetry

■ Extracting Depth

- To extract information about depth from photographs we need multiple perspectives. The **triangulation of stereovision**, allows for computation of depth in the a similar way to that of the human eyes

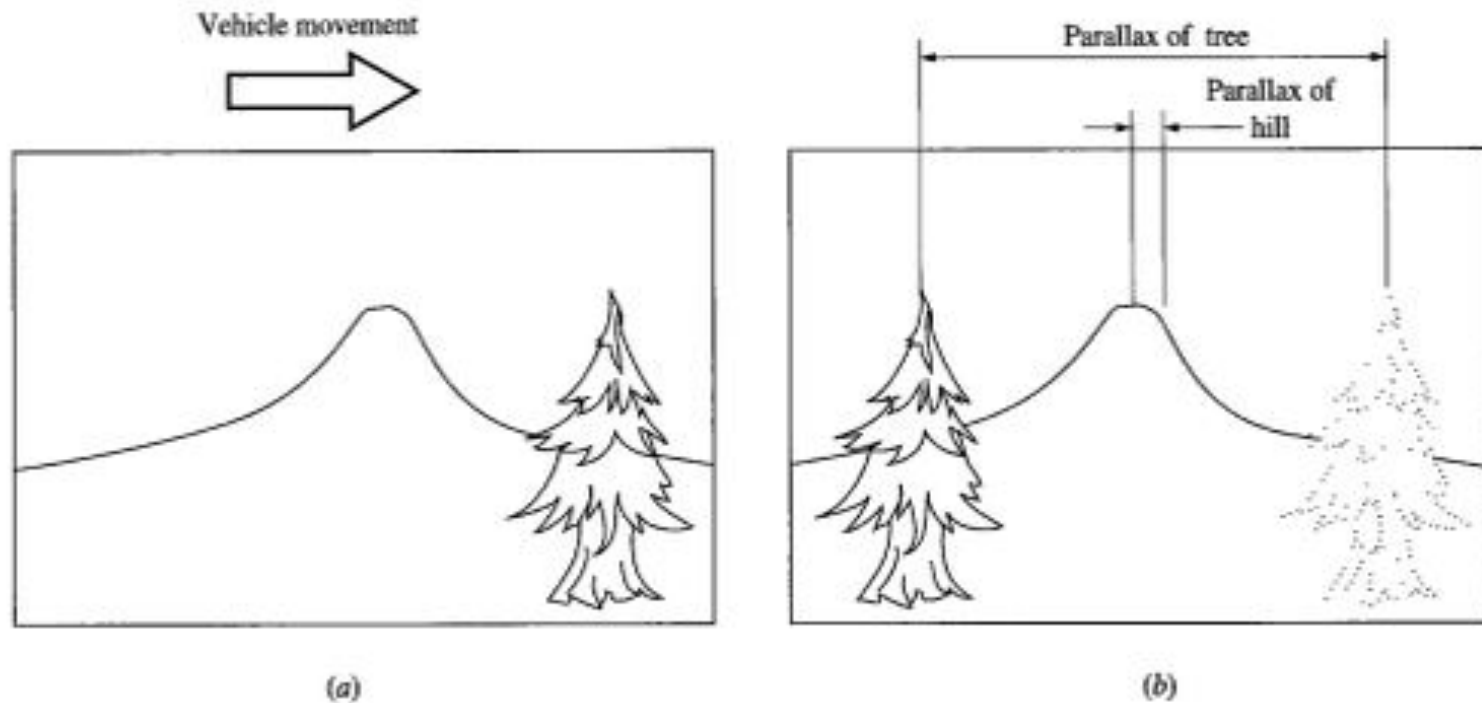


(Source: Introduction to Modern Photogrammetry)

Photogrammetry

■ Extracting Depth

- The concept of **parallax** is another way to interpret depth from photographs. Parallax is the relative relationship between distance from perspective, and movement. (I.E.) an object farther away move much slower than objects close by. Parallax and proximity are inversely related. By studying the movement of **key points** with respect to time the program is able to establish a sense of relative depth.



(Source: Introduction to Modern Photogrammetry)

Photogrammetry

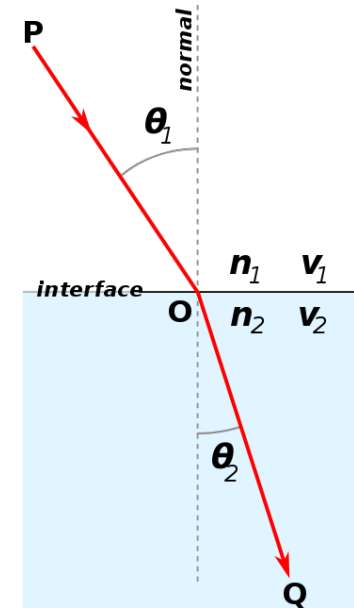
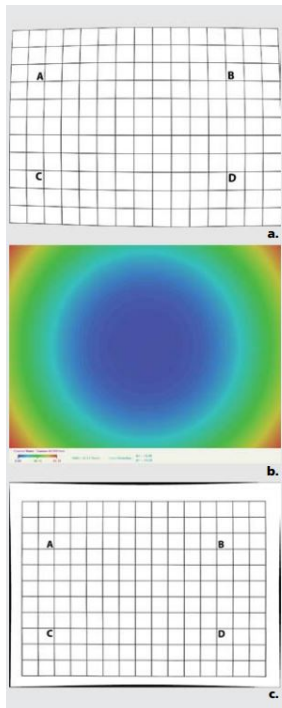
■ Snells law (refraction) distortion, and resolution

- The software's modeling computation must also take into account problems which arise from the refraction of light as it enters the medium of the lens. This refraction modeled after **snells law** must be corrected for. Certain lenses also have fisheye (**radial distortion**), and all have their own **resolution**. The better camera on the UAV, the better the results will be when the software computes the 3D model.

$$\frac{\sin \theta_1}{\sin \theta_2} = \frac{v_1}{v_2} = \frac{\lambda_1}{\lambda_2} = \frac{n_2}{n_1}$$

(Snells Law)

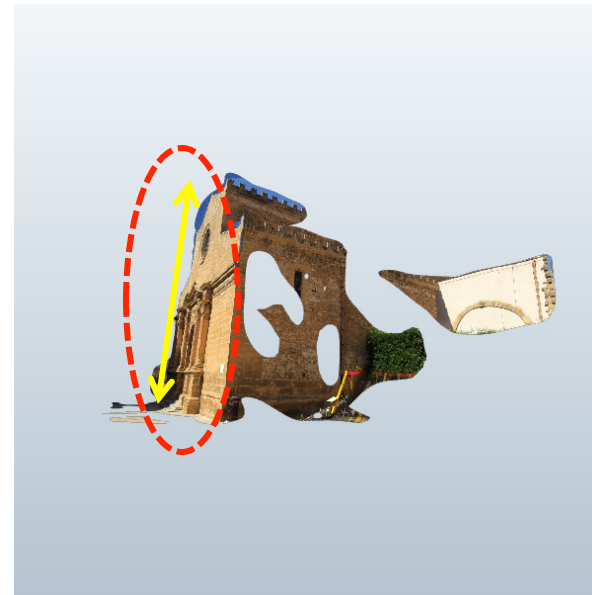
Resolution is the ability to distinguish two light sources from another and an image background. It is a representation of the amount of information stored in the image. A high resolution image will contain more pixels, data, and information per square inch.



Photogrammetry

■ Calibration of the models scale

- In order to correctly analyze any of the 3D information found through photogrammetric approaches, a definite scale needs to be implemented. This means correctly defining a known length and defining it in the model.
- By defining one length, we can thereby define the scale as the aspect ratio of the model is fixed and accurate.



(Source: 123D Catch model gallery)

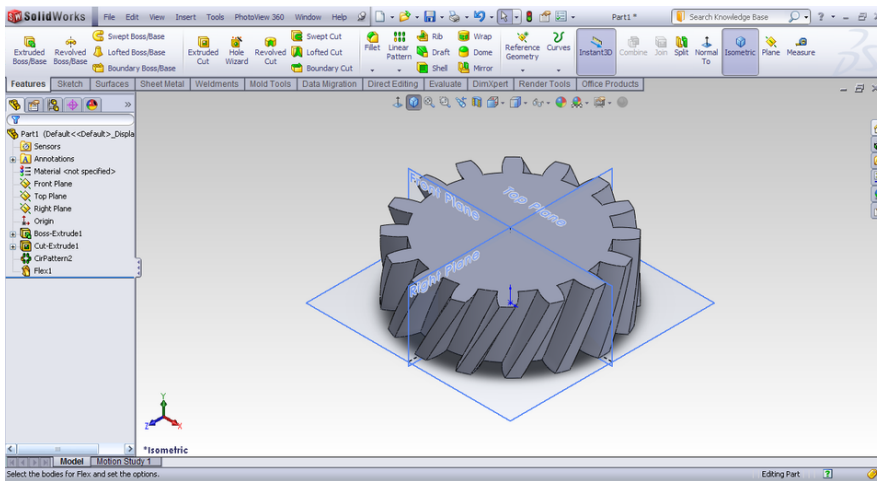
Photogrammetry

- **Software Packages**
 - **123D-Catch (Autodesk)™** photoscanning photogrammetric point cloud generating software, non-commercial
 - **Agisoft Photoscan™** photoscanning photogrammetric point cloud generating software, commercial
 - **Meshlab™** open-source software that allows for qualitative and quantitative evaluation of point cloud and mesh models
 - **Cloud Compare™** open-source software that allows for qualitative and quantitative evaluation of point cloud and mesh models

Photogrammetry

- **Solidworks Models**

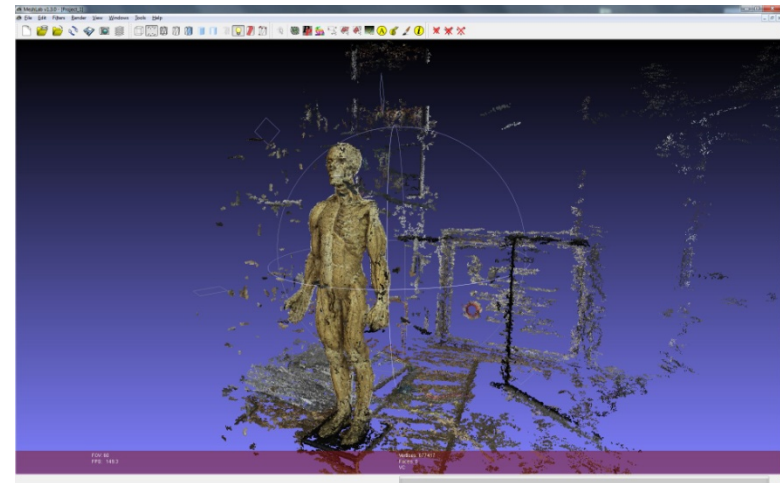
- Provide a more naïve model for analysis



(Source: Solidworks tutorial)

- **Point Cloud and Mesh Models**

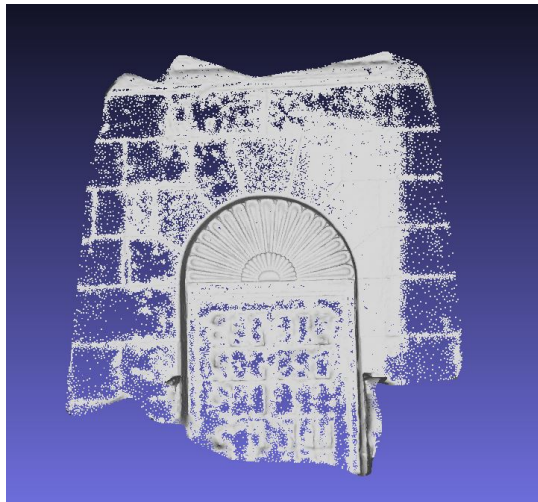
- Provide geometrically accurate models



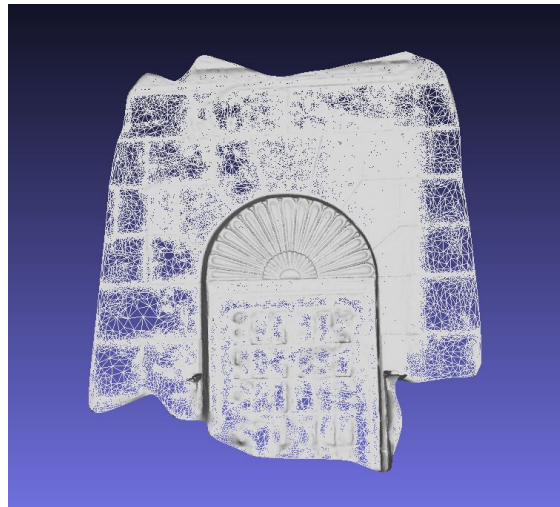
(Source: Syracuse university design works)

Photogrammetry

- **What is a Point Cloud?**
 - Once the computation for relative perspective locations start to calibrate, and **keypoints** are aligned. The software will place points in a relative 3D space which will make up what is referred to as a point cloud model. Triangular mesh from the relationship between points is a **Mesh model**. And by adding a “texture” of the relative images we establish the **final model**.



Point Cloud



Mesh

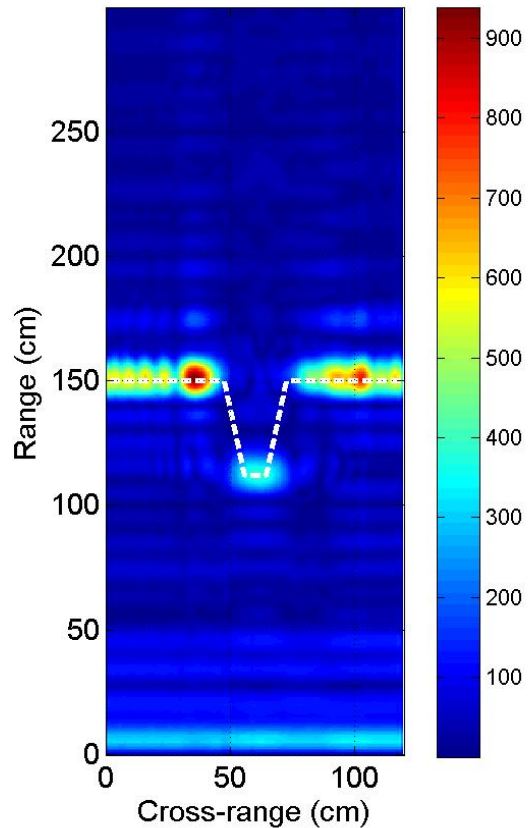


Final

(Source: 123D catch model gallery)

Other Approaches (SAR)

- **Synthetic Aperature Radar Imaging is :**
A subsurface imaging process based on the relative amplitudes of reflected microwave responses.

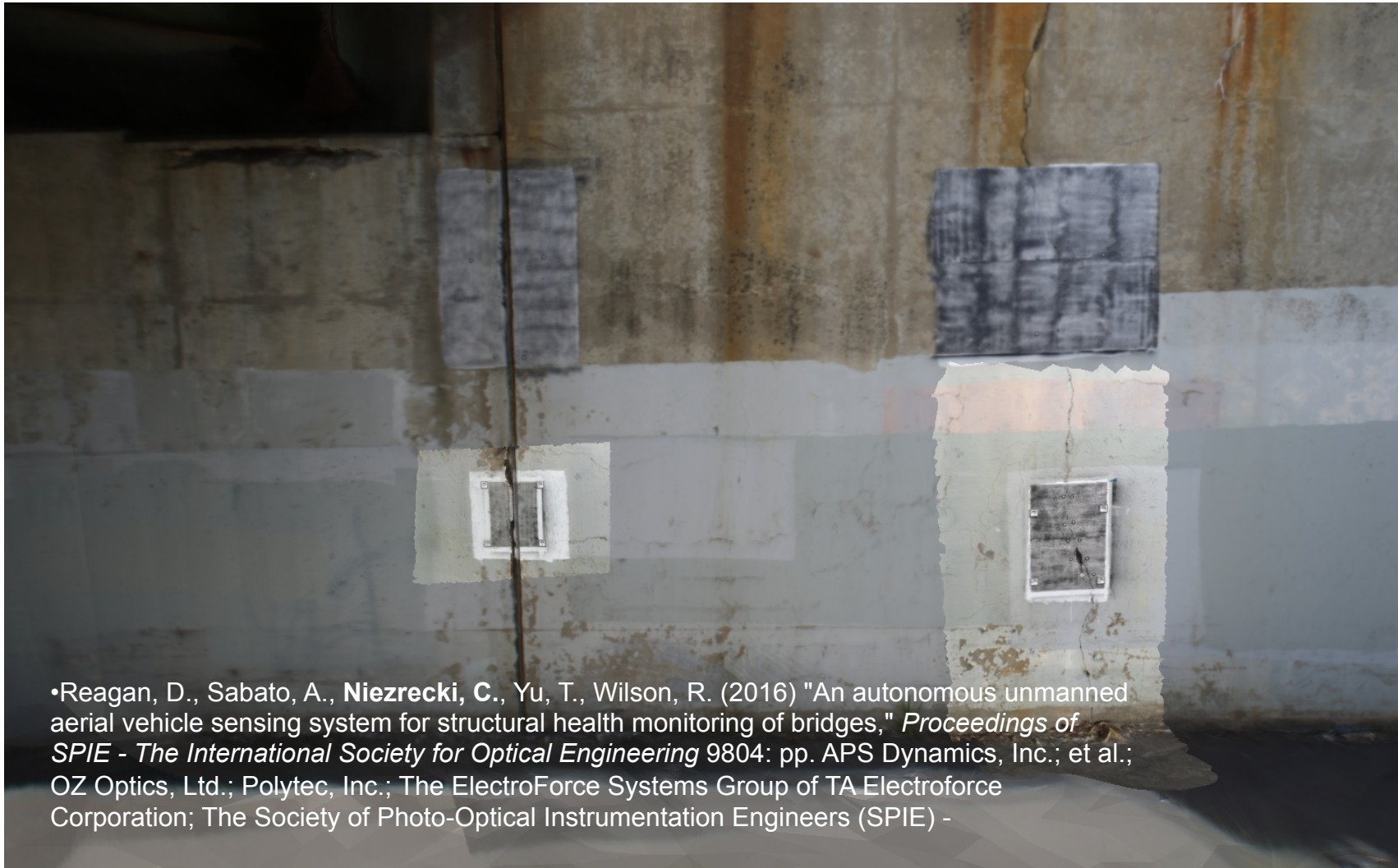


Yu, T., J. Owusu-Twumasi, V. Le, Q. Tang, D'Amico N, (2016), "Surface and Subsurface Remote Sensing of Concrete Structures using Synthetic Aperture Radar Imaging", *ASCE, Journal of Structural Engineering (Accepted)*

Background (DIC)

- **Digital Image Correlation:**

A photogrammetric method for calculating strain information.

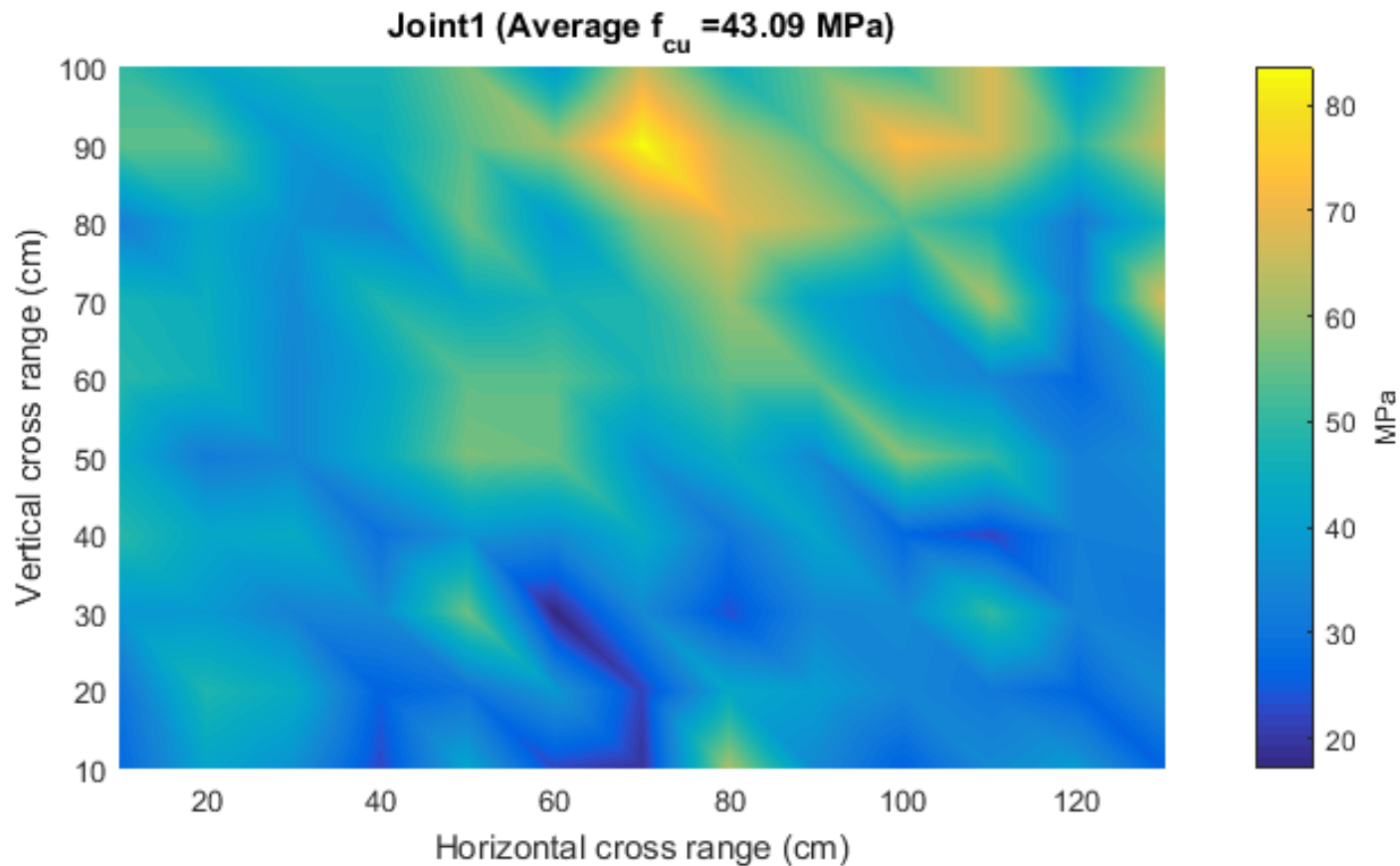


•Reagan, D., Sabato, A., **Niezrecki, C.**, Yu, T., Wilson, R. (2016) "An autonomous unmanned aerial vehicle sensing system for structural health monitoring of bridges," *Proceedings of SPIE - The International Society for Optical Engineering* 9804: pp. APS Dynamics, Inc.; et al.; OZ Optics, Ltd.; Polytec, Inc.; The ElectroForce Systems Group of TA Electroforce Corporation; The Society of Photo-Optical Instrumentation Engineers (SPIE) -

Other Approaches (RBH)

- **Rebound Hammer:**

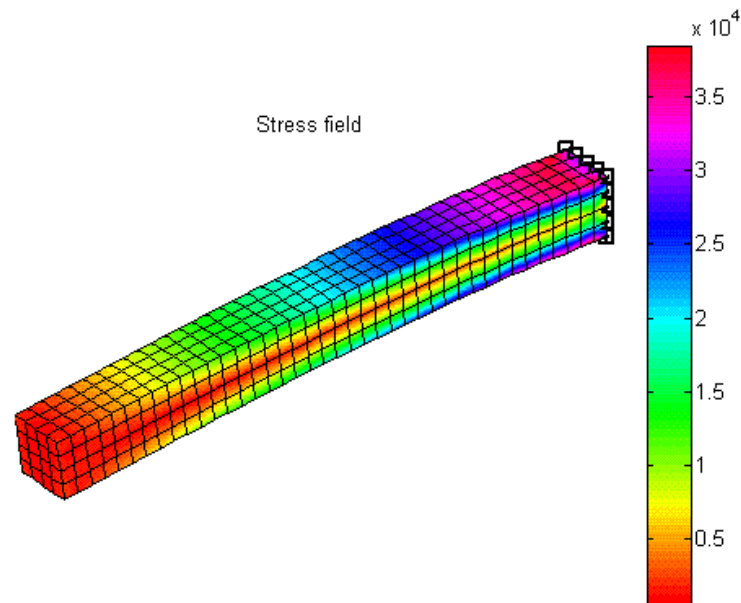
An acoustic NDE technique for locating areas of damage in structures.



Background

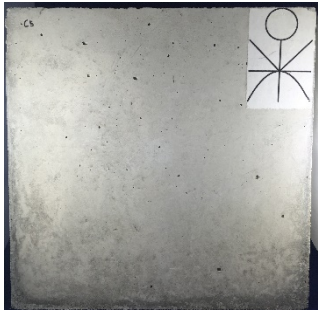
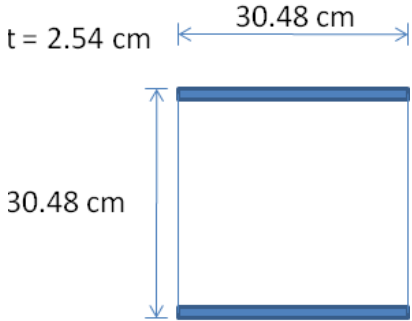
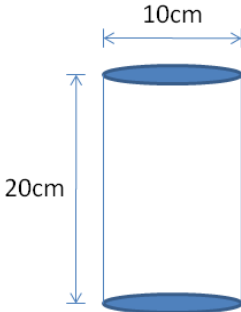
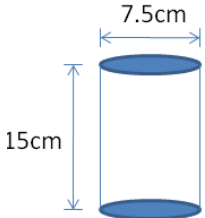
- **Finite Element Modeling is :**

Constructing a model of finitely defined mesh sections for numerical analysis.



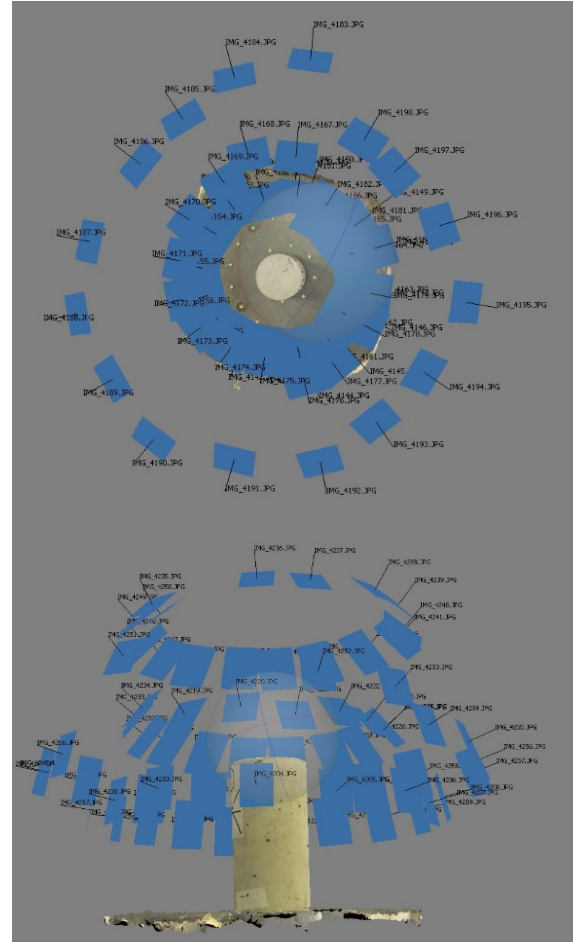
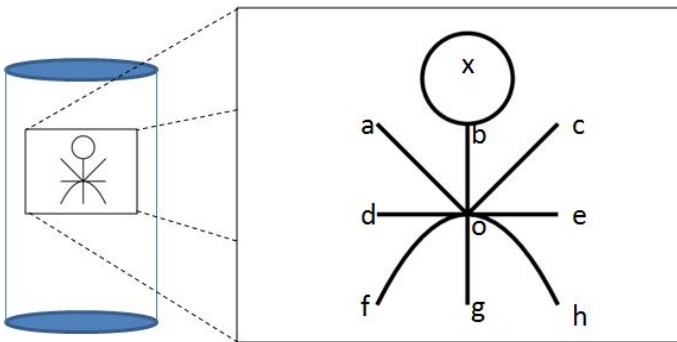
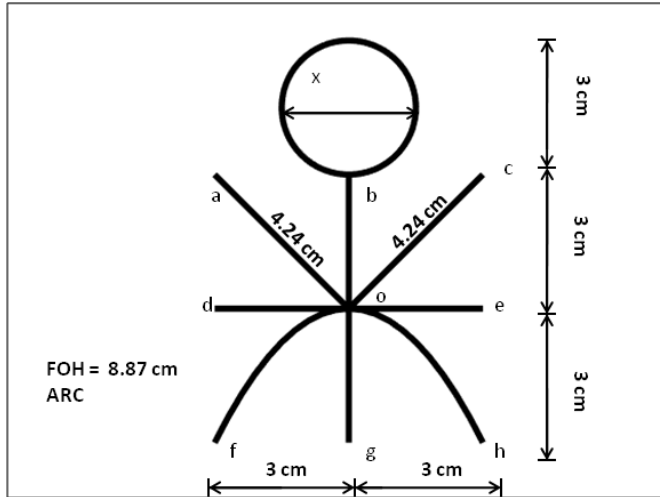
Methodology

- Lab Specimens



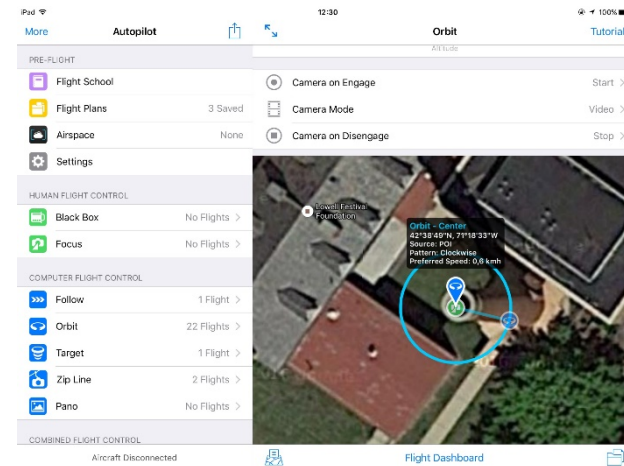
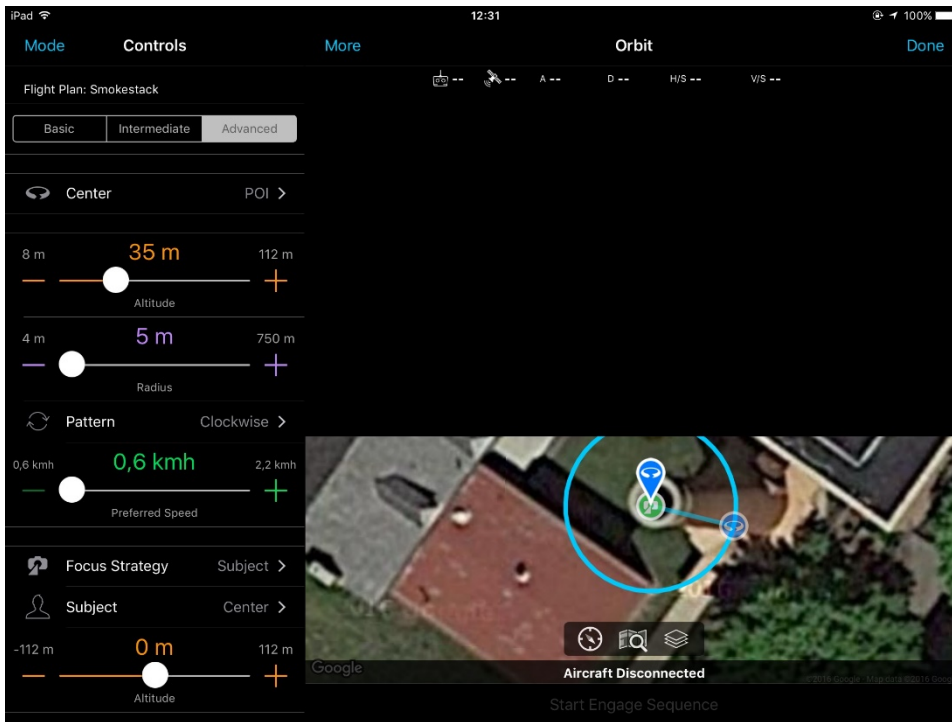
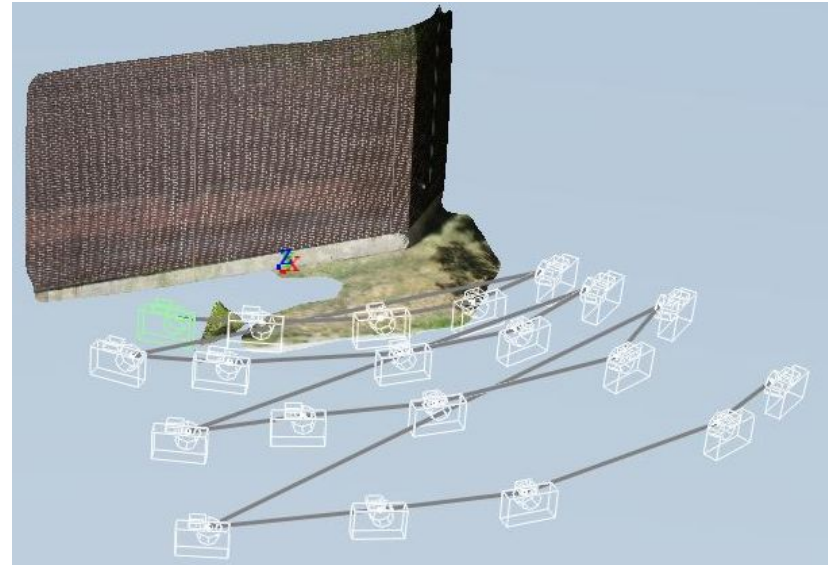
Methodology

- The setup for data acquisition is shown below:



Methodology

- In-Situ acquisition scheme
 - Terrestrial
 - UAV airborne

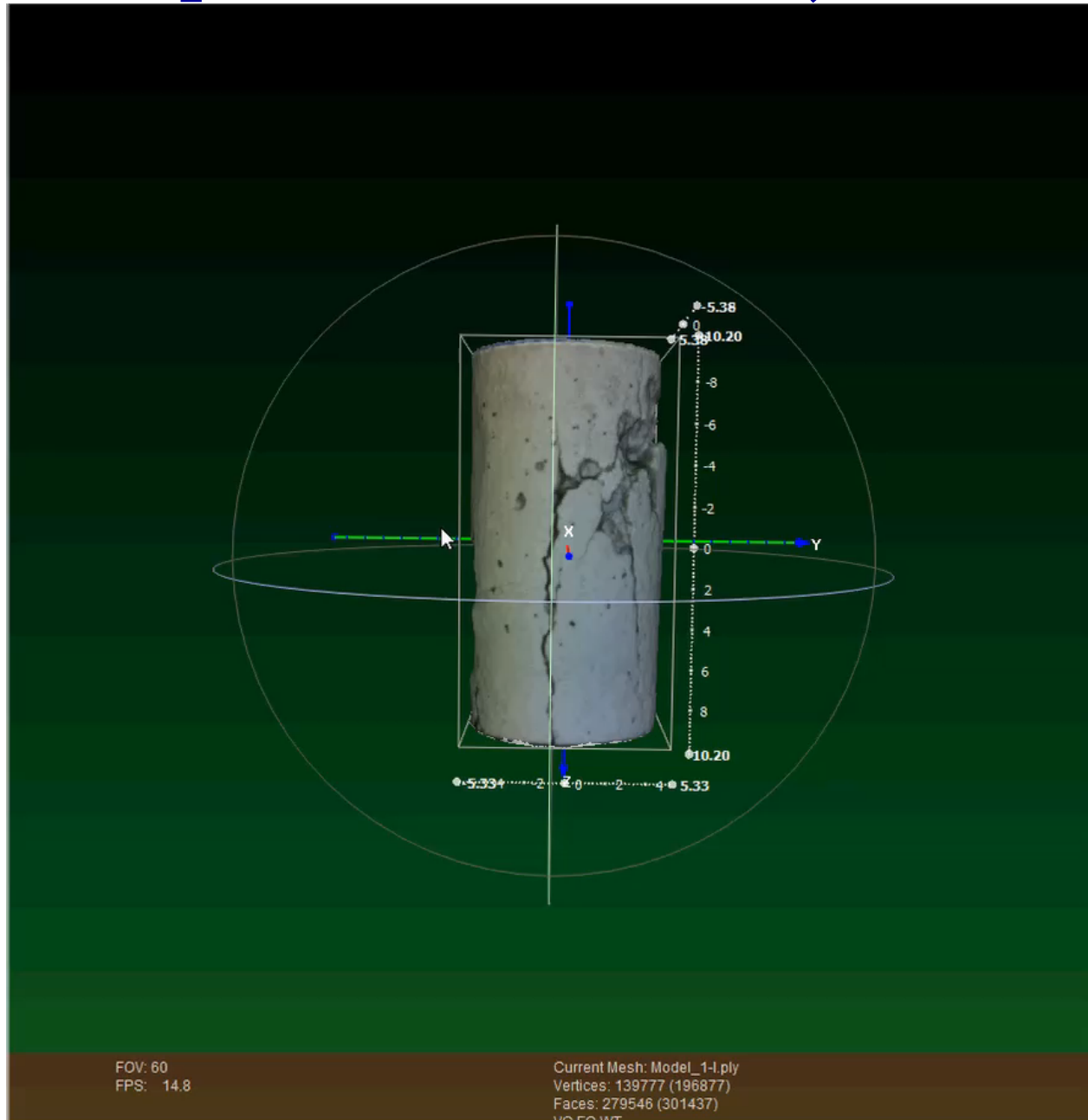


Methodology

- **In-Situ acquisition scheme**
 - **Terrestrial**
 - **UAV airborne**

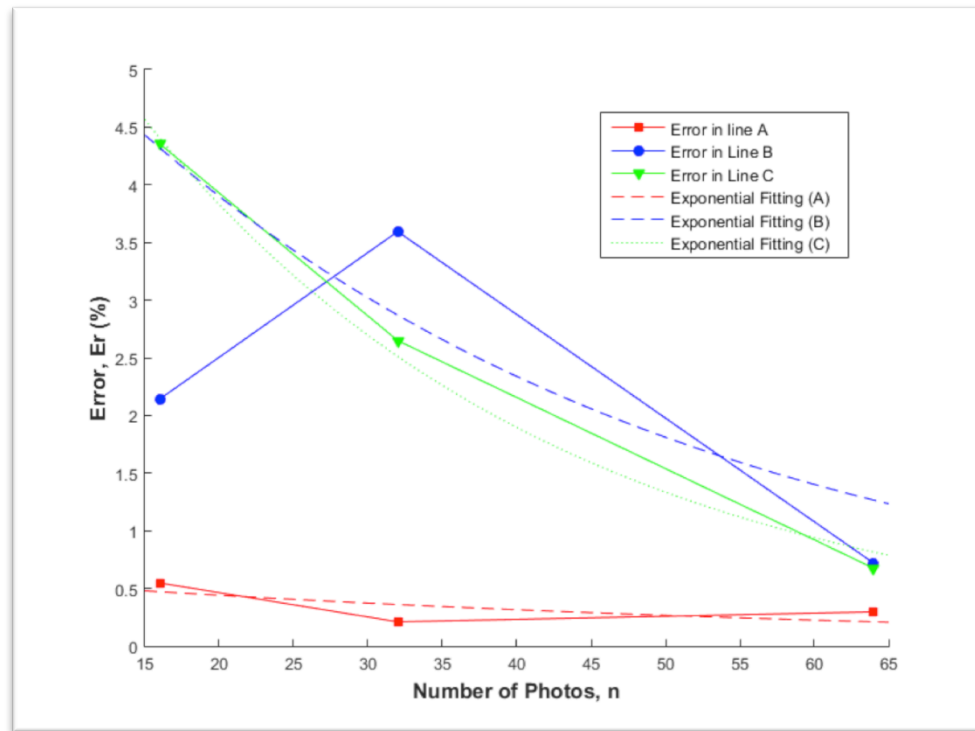
- **VIDEO ON THIS SLIDE WAS TOO LARGE TO SEND**
- **(its an autopilot demonstration using the UAV)**

Lab Specimen Results (Geometric)



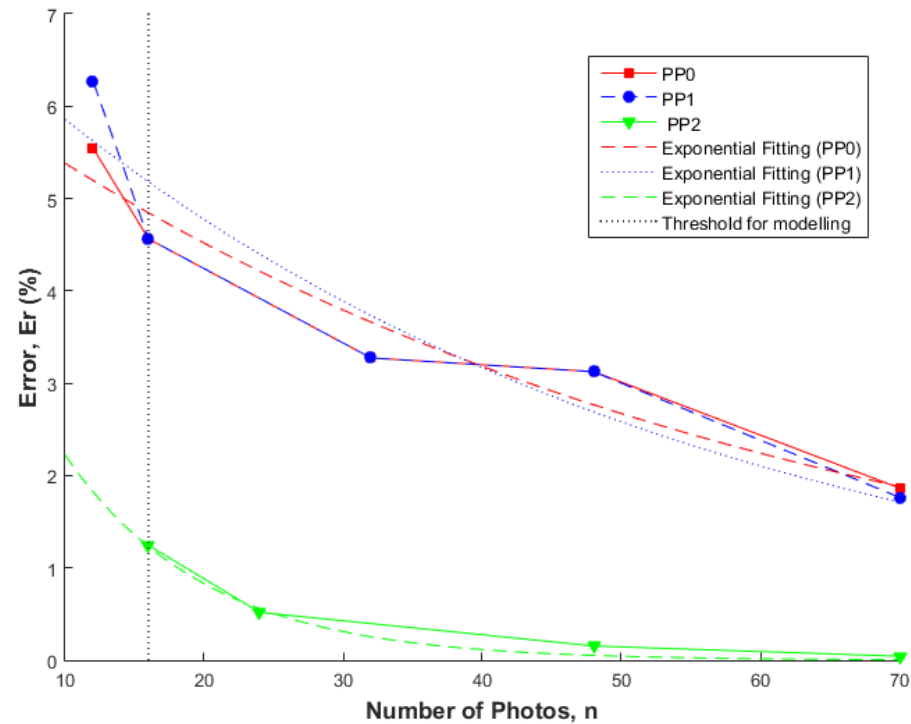
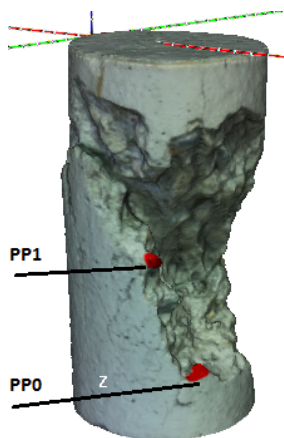
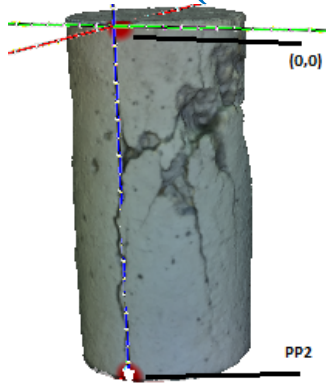
Lab Specimen Results (Geometric)

- Examples of Evaluative Techniques (Localization)



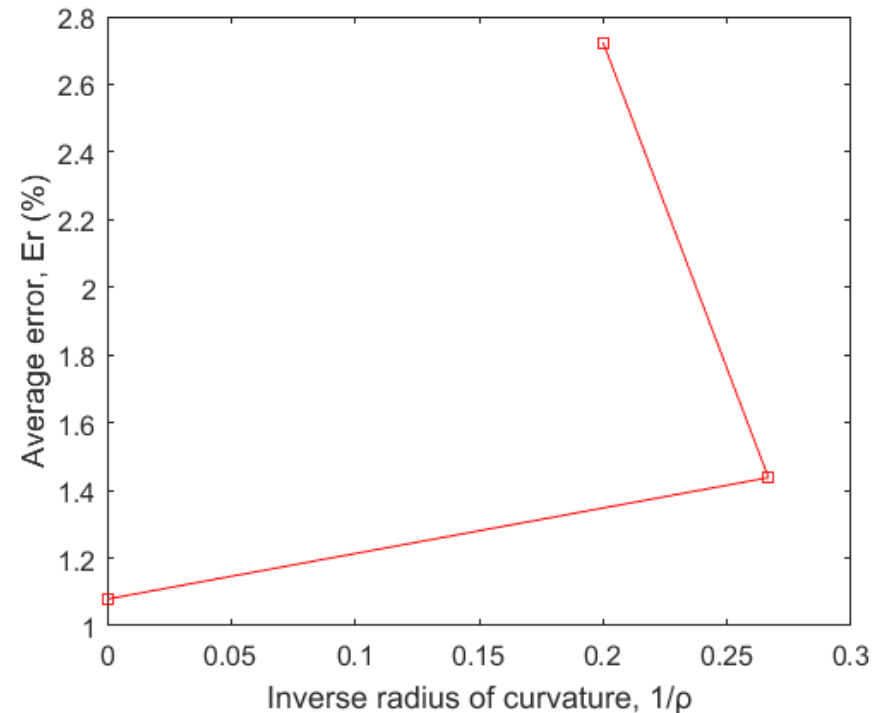
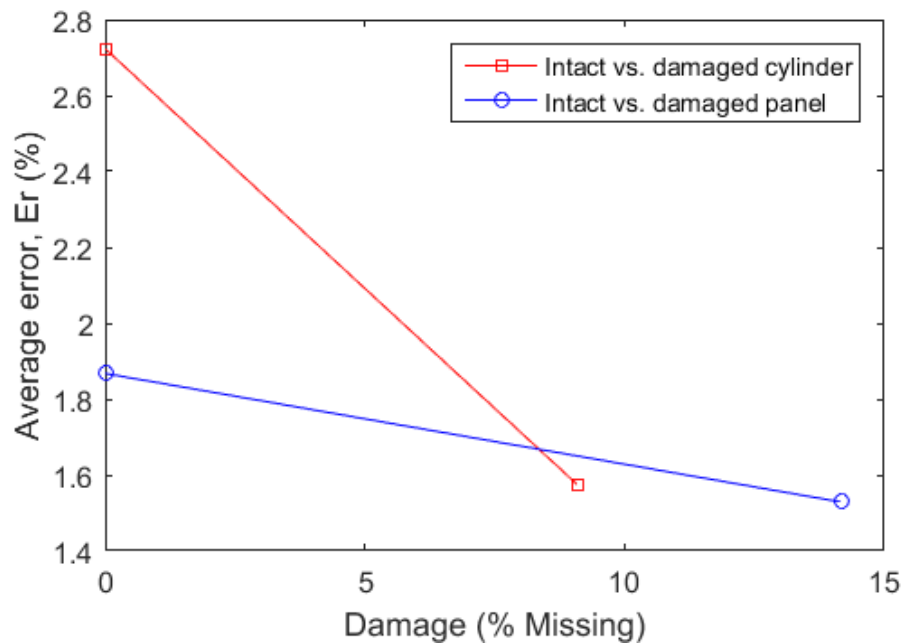
Lab Specimen Results (Geometric)

■ Examples of Evaluative Techniques (Localization)

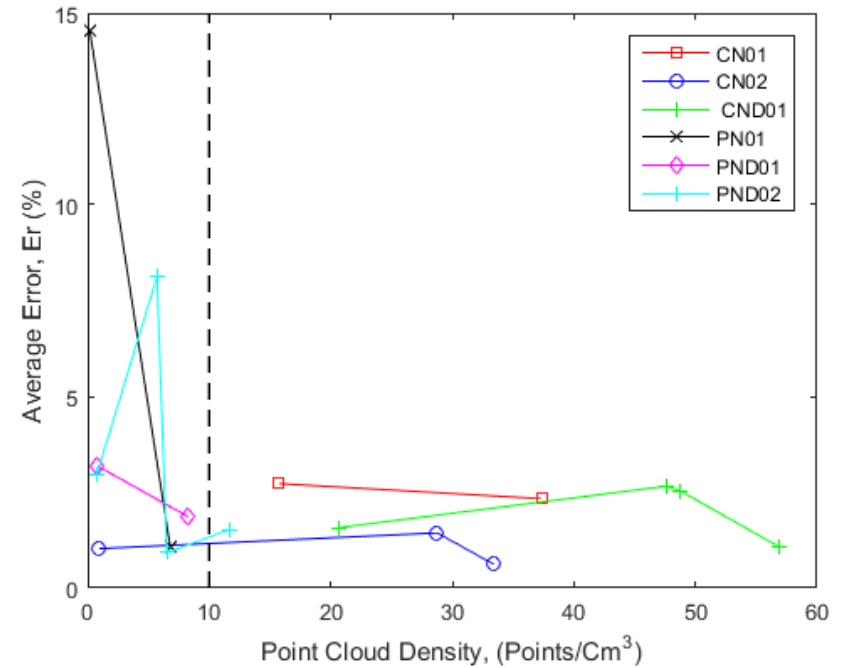
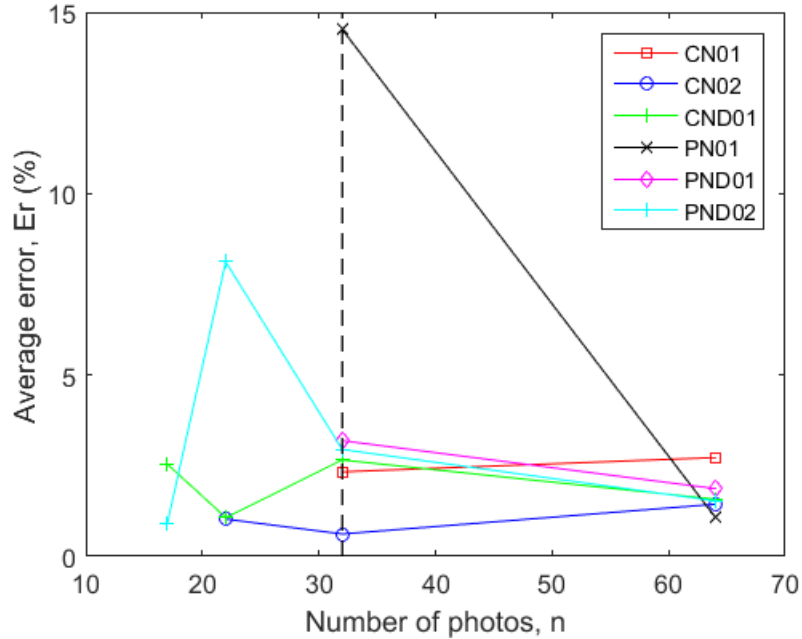


Lab Specimen Results (Geometric)

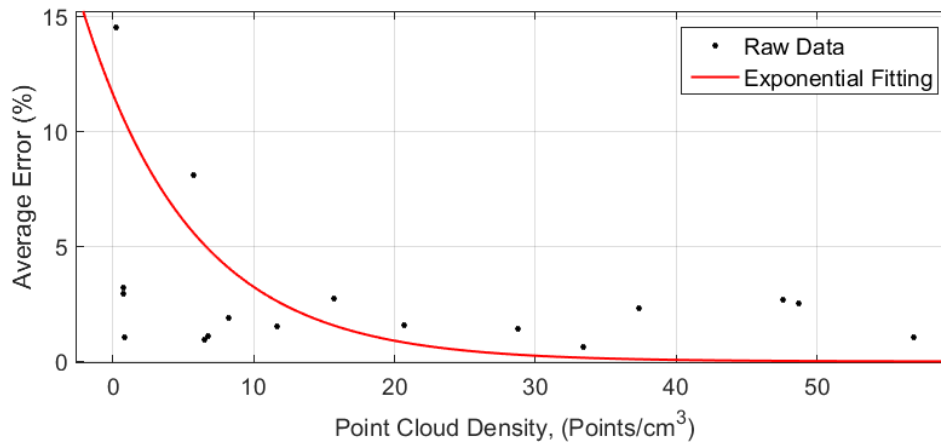
- Some of our results are shown below
- Damage trend was expected
- Curvature was not



Lab Specimen Results (Geometric)

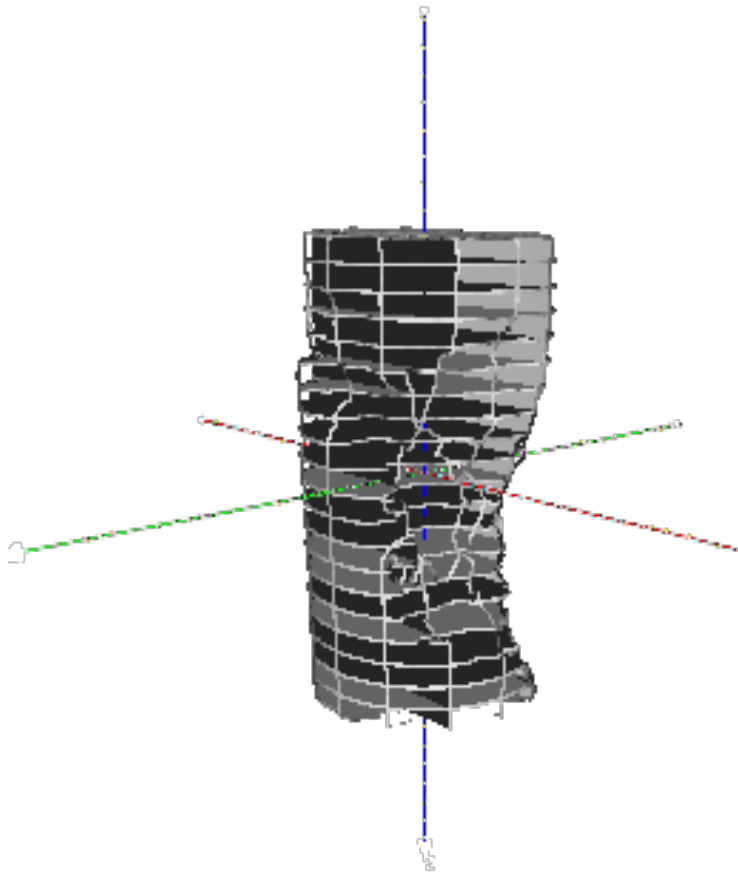


A threshold point cloud density (PCD) of **15.7194 Pts/cm³** is proposed for constructing a reliable accurate model for condition assessment.



Lab Specimen Results (Geometric)

- Examples of Evaluative Techniques (volume, x-sects and Stress evaluation)

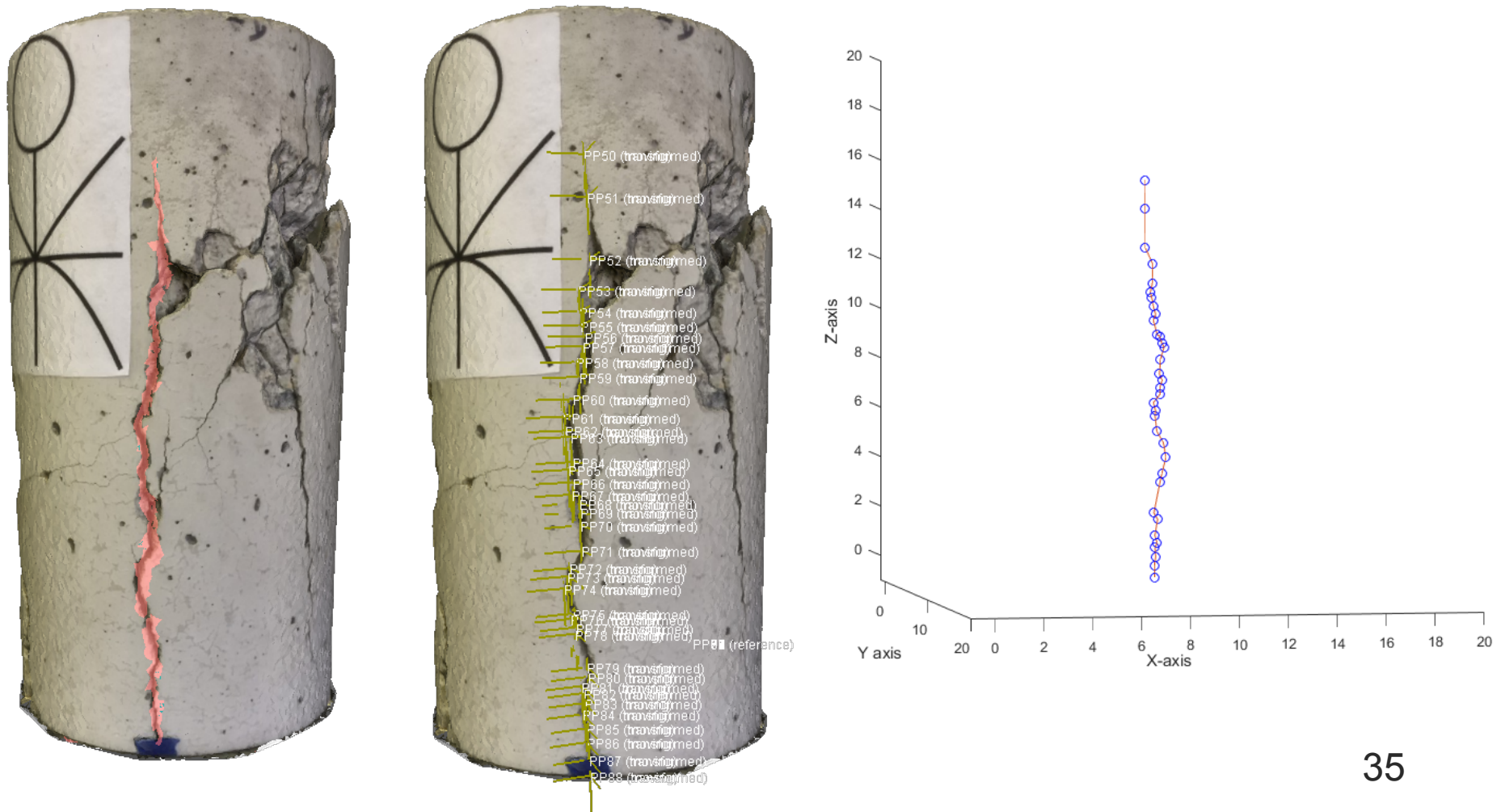


	P(N)	Az(adj) (m2)	σ (adj) (Pa)
Z(-10)	1	0.003605755	277.3343937
Z(-9)	1	0.007898969	126.5988013
Z(-8)	1	0.007858712	127.2473224
Z(-7)	1	0.007691608	130.0118255
Z(-6)	1	0.007372336	135.6422158
Z(-5)	1	0.00702173	142.4150363
Z(-4)	1	0.006845186	146.0880697
Z(-3)	1	0.006760788	147.9117416
Z(-2)	1	0.006370679	156.9691495
Z(-1)	1	0.006237504	160.3205348
Z(0)	1	0.006028885	165.8681568
Z(1)	1	0.005716305	174.9381784
Z(2)	1	0.005622775	177.8481166
Z(3)	1	0.005844754	171.0936013
Z(4)	1	0.00603487	165.7036636
Z(5)	1	0.006272665	159.4218663
Z(6)	1	0.00662056	151.0446233
Z(7)	1	0.007073605	141.37063
Z(8)	1	0.007336813	136.2989641
Z(9)	1	0.007631933	131.0284051
Z(10)	1	0.006475494	154.4283659

Vm (Cm3)	1436.946899
Vv (Cm3)	1369.84784
Vin (Cm3)	1570.796327
ΔV_v (Cm3)	200.9484868
ΔV_m (Cm3)	133.8494278
Erm (%)	4.898285564
Damv(%)	12.79277799
Damm(%) Mesh	8.521119225

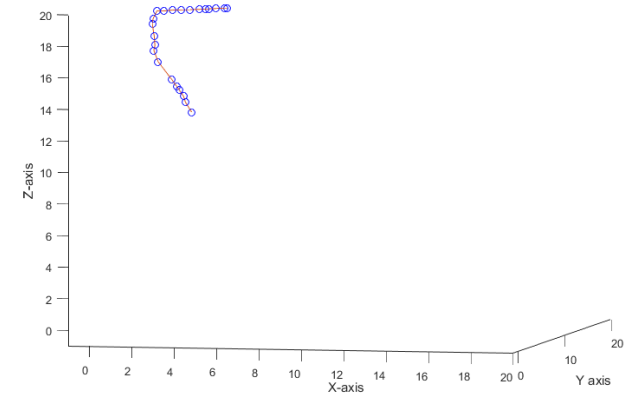
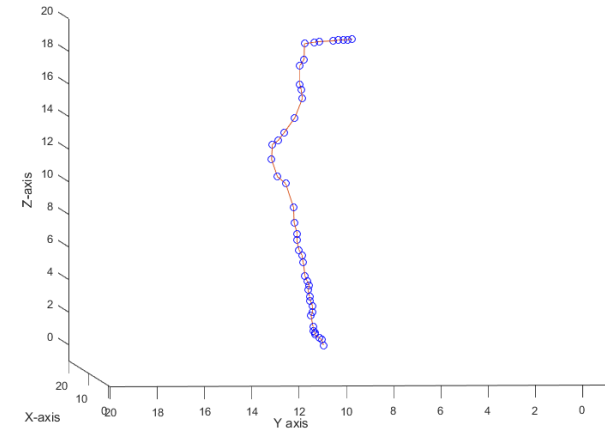
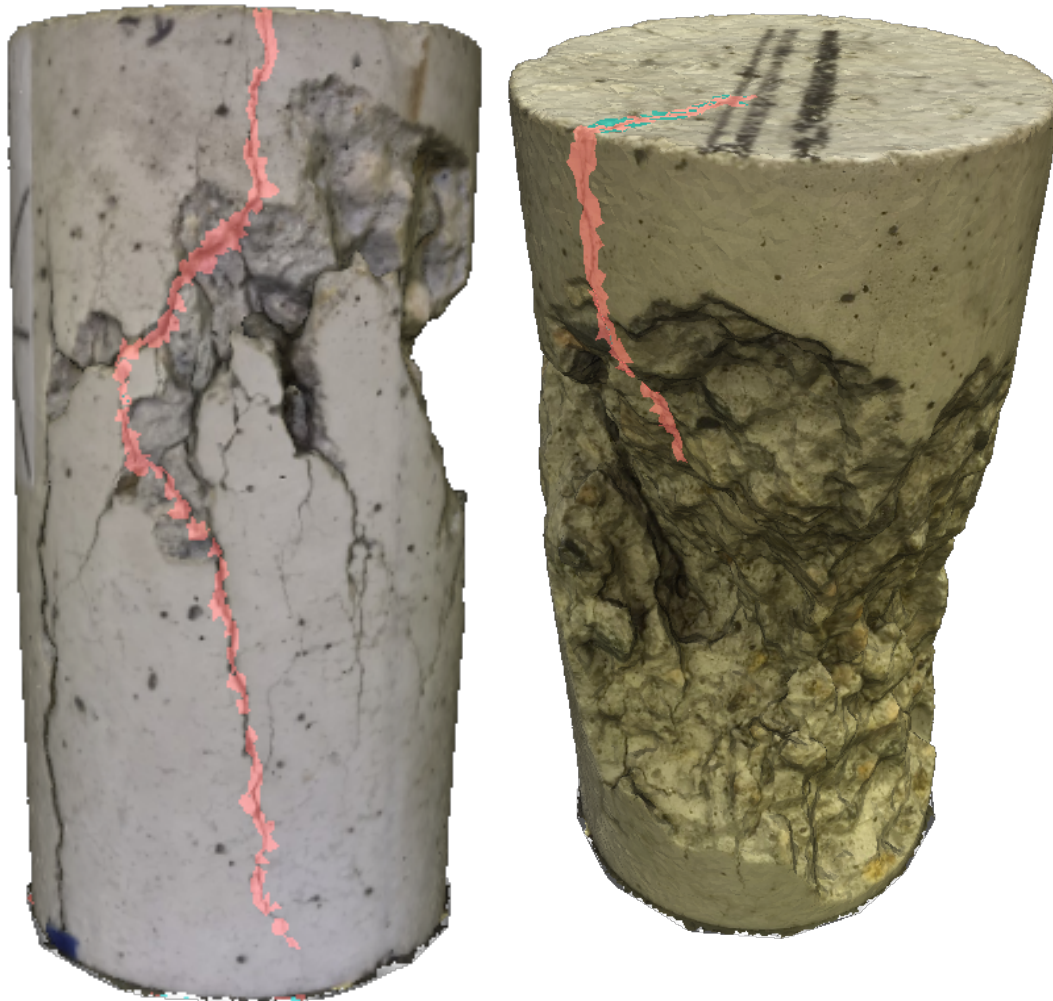
Lab Specimen Results (Surface Crack Profiling)

- Surface Crack Profiling of a damaged specimen



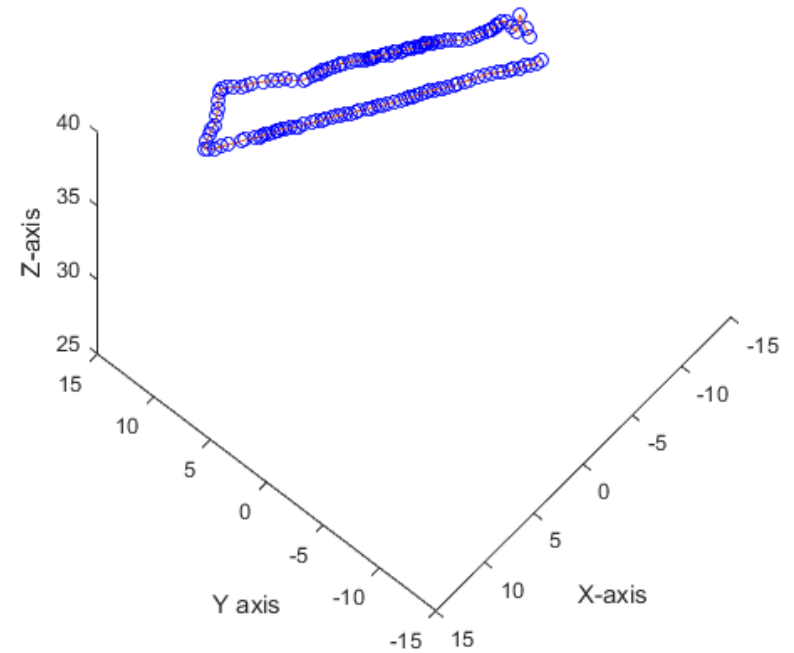
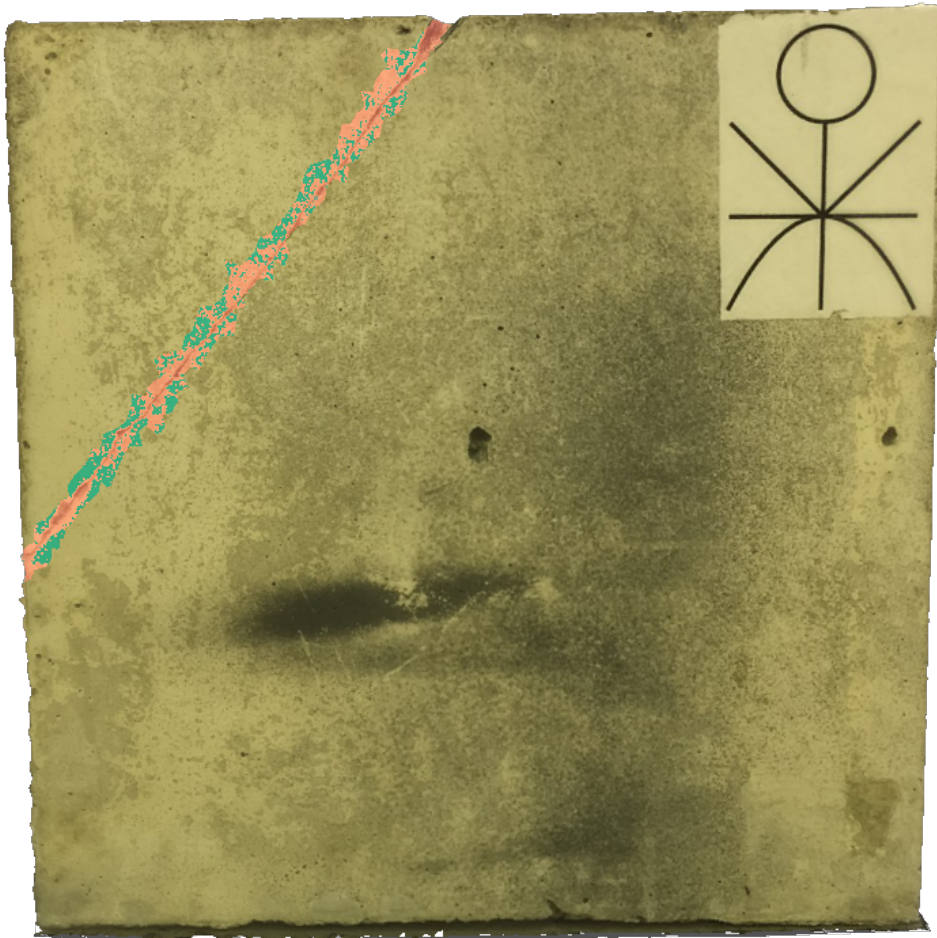
Lab Specimen Results (Surface Crack Profiling)

- Surface Crack Profiling of a damaged specimen



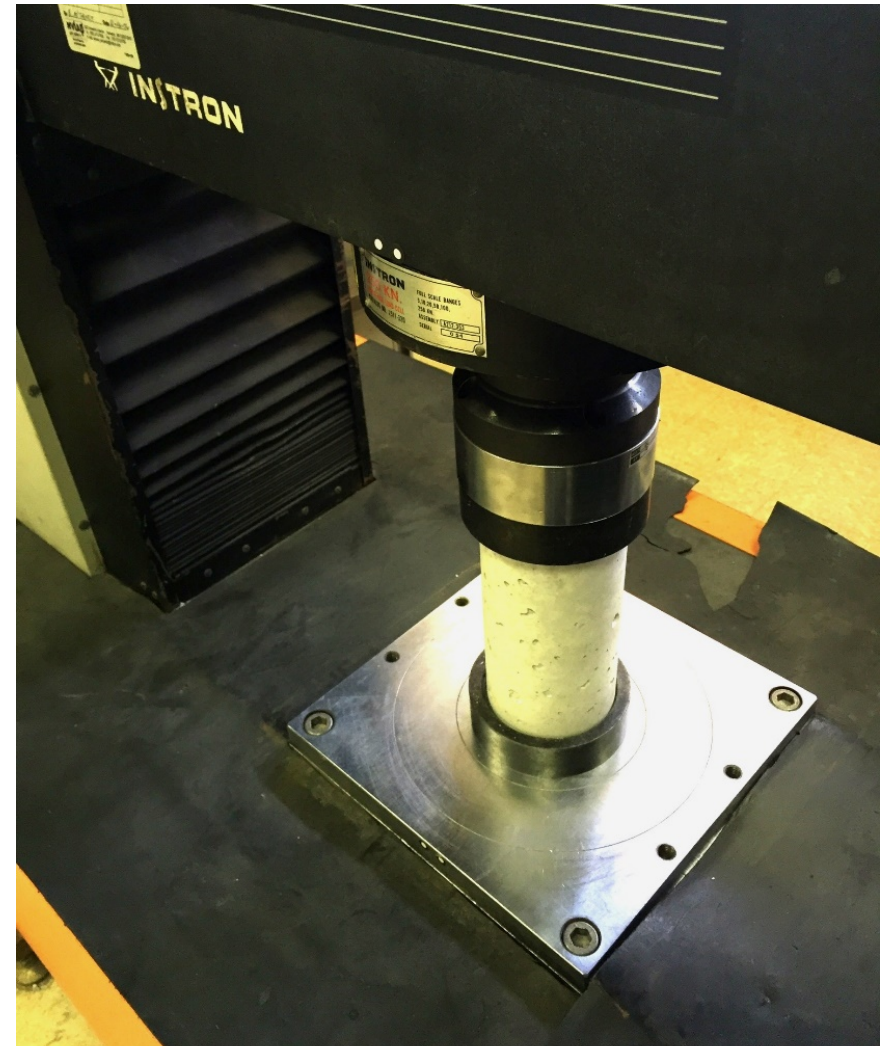
Lab Specimen Results (Surface Crack Profiling)

- Surface Crack Profiling of a damaged specimen



Lab Specimen Results (Mechanical)

- **INSTRON** at UMass Lowell, used to load specimen at 20%, and 40% of ultimate load
- **In accordance with ASTM C469M-14** "Standard Test Method for Static Modulus of Elasticity and Poisson's Ratio of Concrete in Compression".
- **Ultimate load estimated to be 3,750 psi.**



Lab Specimen Results (Mechanical)

- Relative load assessment using lateral strain measurements

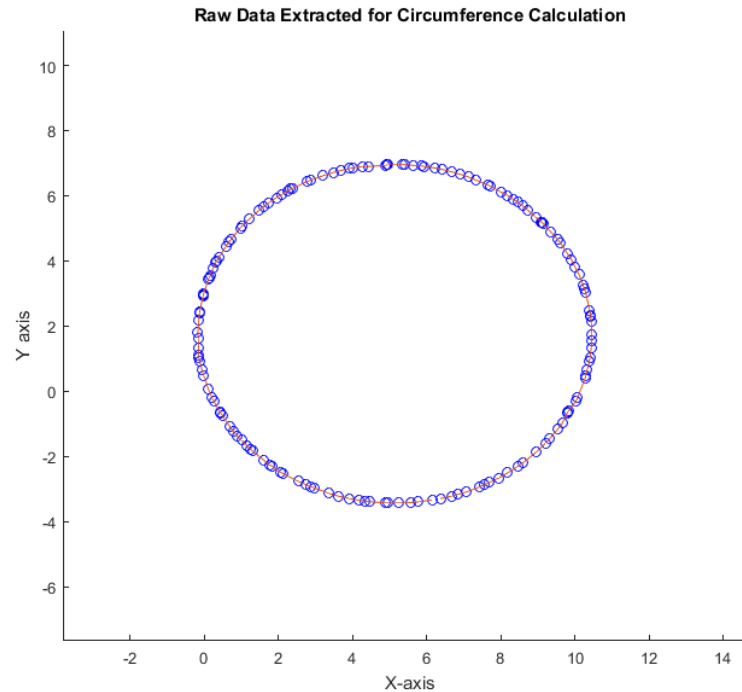
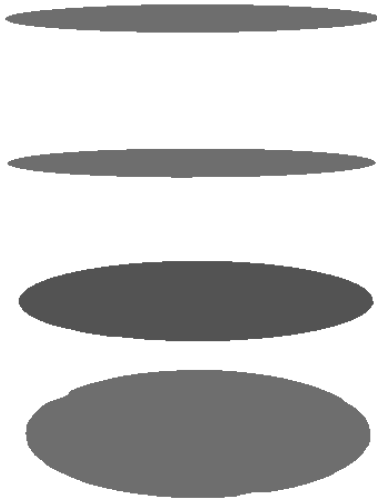


Table 4. Cross sectional surface areas at 0%, 20%, and 40% loading

	0% cm ²	20% cm ²	ΔSA(%)	40% cm ²	ΔSA(%)
Z4	82.409714	82.84245	0.525097	84.17691	2.144403
Z8	83.3246	83.97095	0.775698	85.2244	2.279994
Z12	84.149651	84.94586	0.946185	86.08547	2.300448
Z16	85.00502	85.86791	1.015107	86.75012	2.05294
Avg	83.722246	84.40679	0.817638	85.55922	2.194134

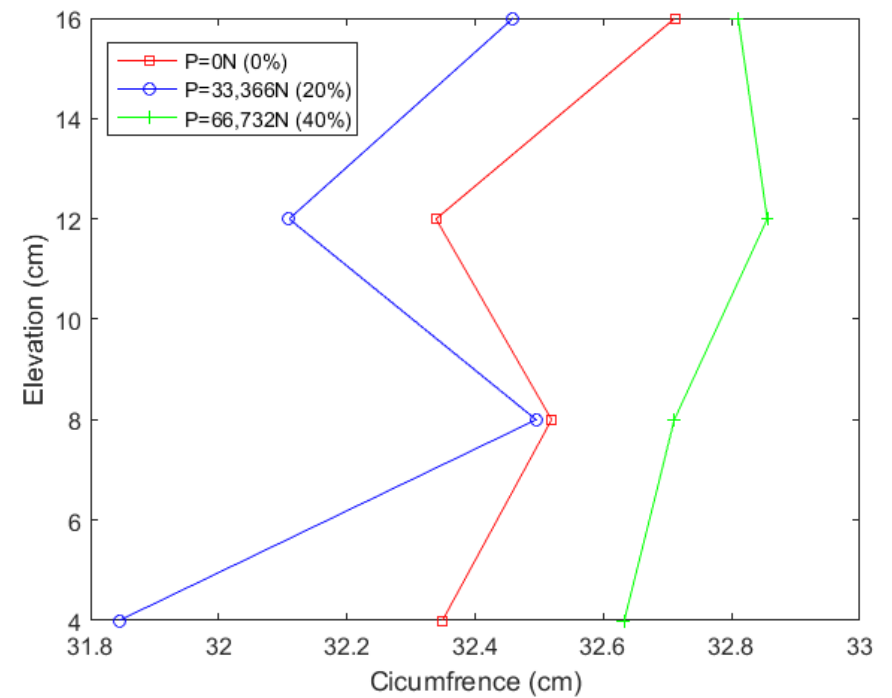
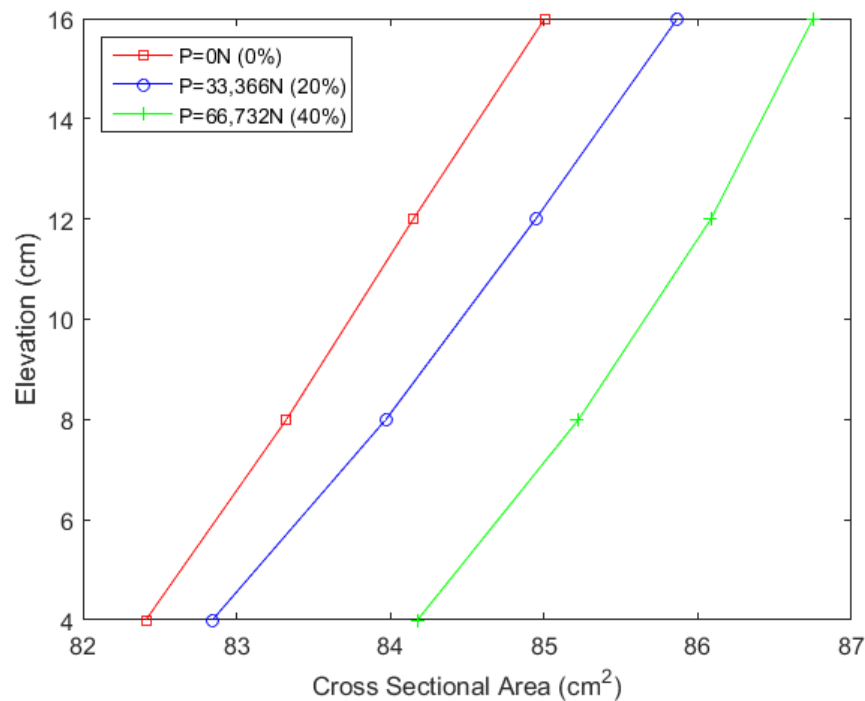
Table 5. Circumference values at 0%, 20%, and 40% loading

	0% cm	20% cm	40% cm
Z4	32.3490	31.8448	32.6327
Z8	32.5192	32.4950	32.7106
Z12	32.3389	32.1098	32.8556
Z16	32.7118	32.4592	32.8102
Avg	32.47973	32.2272	32.75228

Lab Specimen Results (Mechanical)

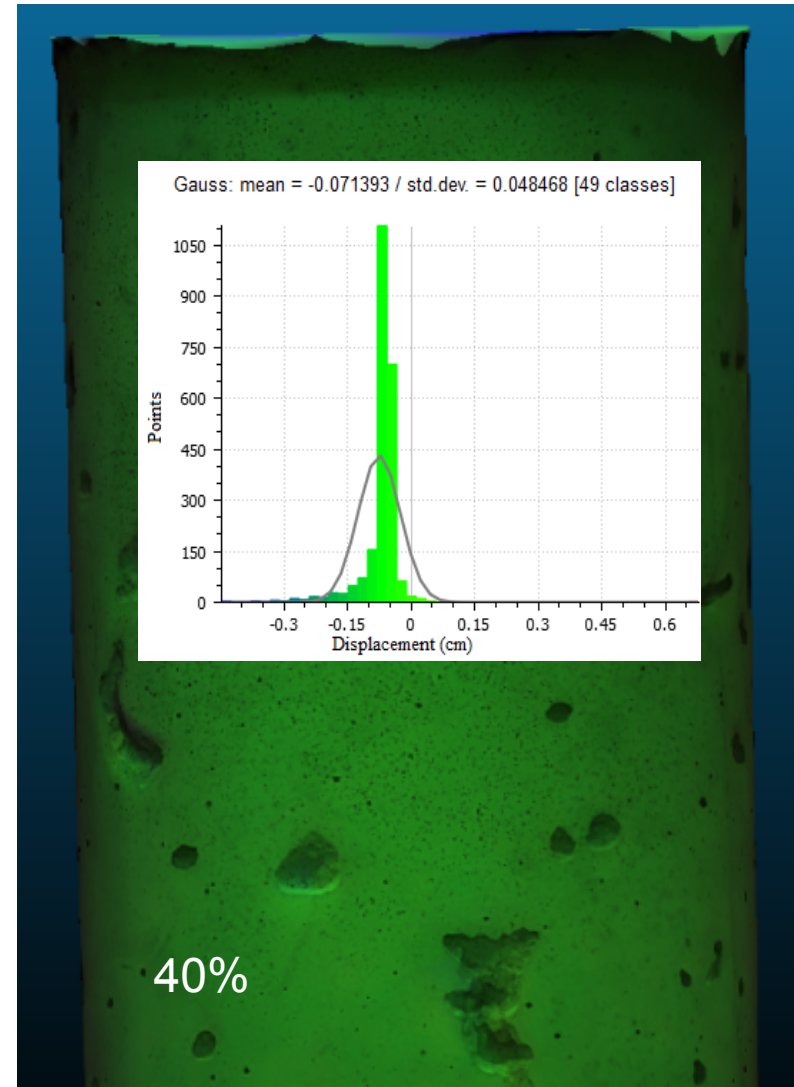
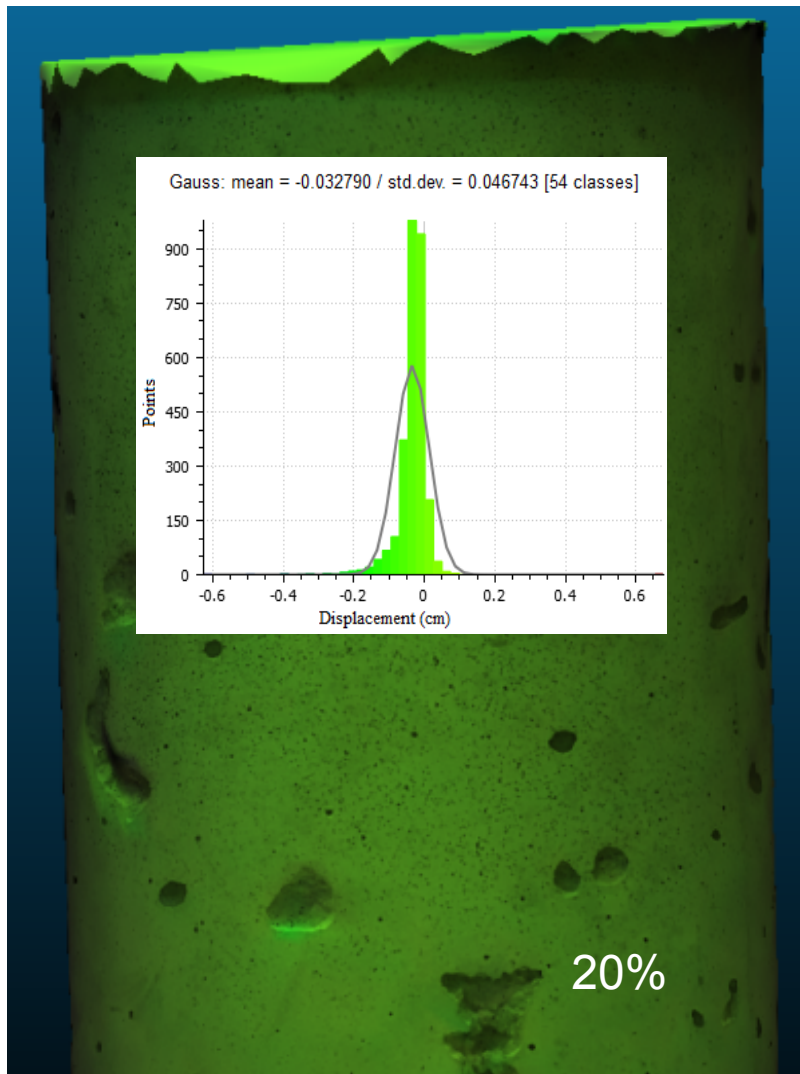
- Relative load assessment using lateral strain measurements

	0% cm^2	20% cm^2	40% cm^2
Diam (d)	10.324654 cm	10.36678 cm	10.43731 cm
Strain (ϵ_L)		0.00408	0.010911



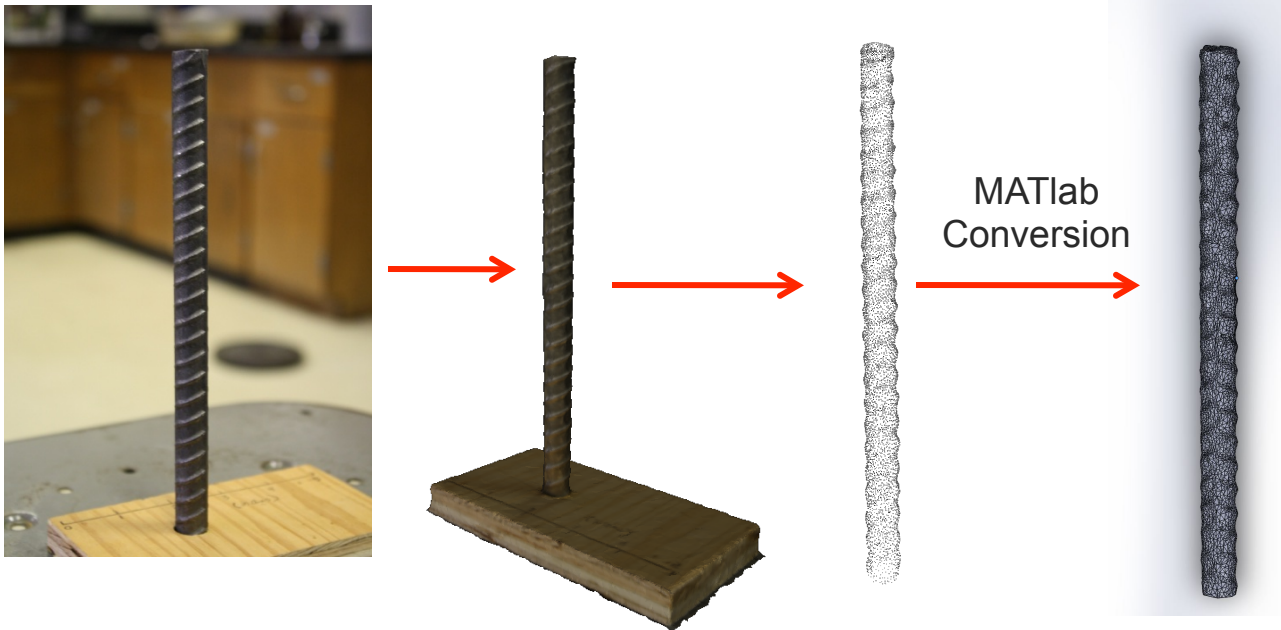
Lab Specimen Results (Mechanical)

- Relative load assessment using ICP A maximum distance of 0.67872399 cm



Lab Specimen Results (FEM)

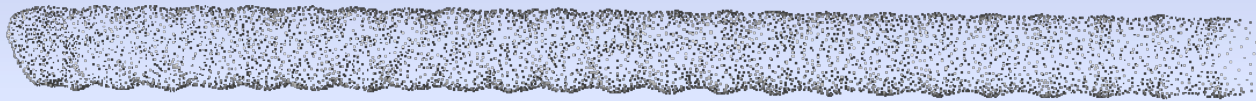
- Rebar Modeling



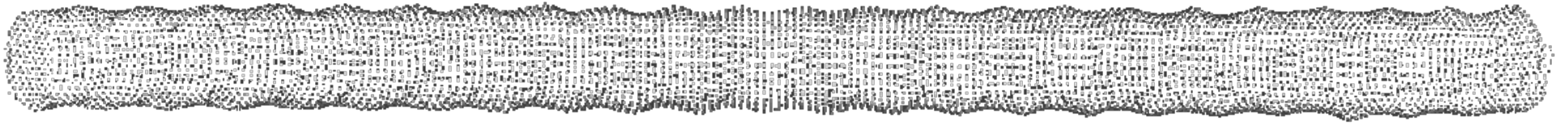
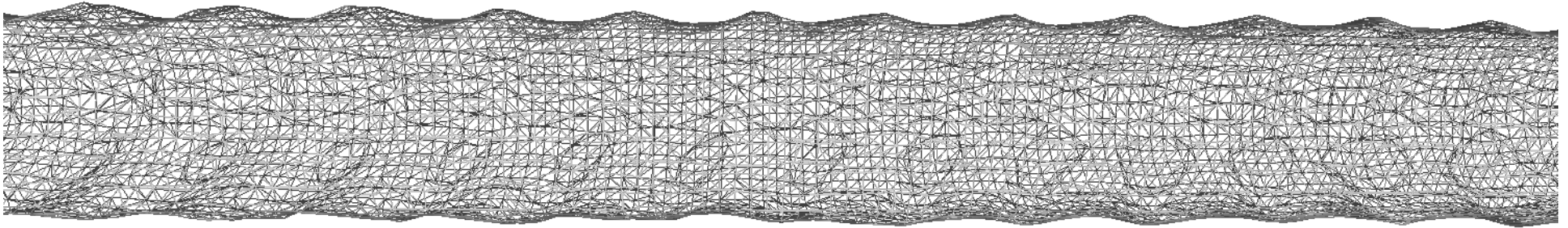
Conversion from photogrammetric model, point cloud information into a CAD applicable solid mesh allows for finite element modeling of a specimen without the sacrifice of geometric variations.

Lab Specimen Results (FEM)

The problem with modeling a FE model from point cloud data is in the irregularity of points. Data needs to be interpolated with a regular dx, dy, dz to make a pure mesh grid



Lab Specimen Results (FEM)



Using uniform resampling technique in Meshlab point cloud processing software the mesh was transformed into a uniform grid.

Then using a matlab function was converted from (.stl)-> (.sat) shell to part

Lab Specimen Results (FEM)

The screenshot displays the Abaqus/CAE 6.14-1 software interface. The main window shows a 3D view of a cylindrical specimen with a green mesh. The specimen is oriented along the X-axis. The coordinate system (X, Y, Z) is visible in the 3D view. The left-hand side contains a Model Database tree with the following structure:

- Model Database
 - Models (1)
 - Model-1
 - Parts (1)
 - Materials
 - Calibrations
 - Sections
 - Profiles
 - Assembly
 - Steps (1)
 - Field Output Requests
 - History Output Requests
 - Time Points
 - ALE Adaptive Mesh Constraints
 - Interactions
 - Interaction Properties
 - Contact Controls
 - Contact Initializations
 - Contact Stabilizations
 - Constraints
 - Connector Sections
 - Fields
 - Amplitudes
 - Loads
 - BCs
 - Predefined Fields
 - Remeshing Rules
 - Optimization Tasks
 - Sketches
 - Annotations
 - Analysis
 - Jobs
 - Adaptivity Processes
 - Co-executions
 - Optimization Processes

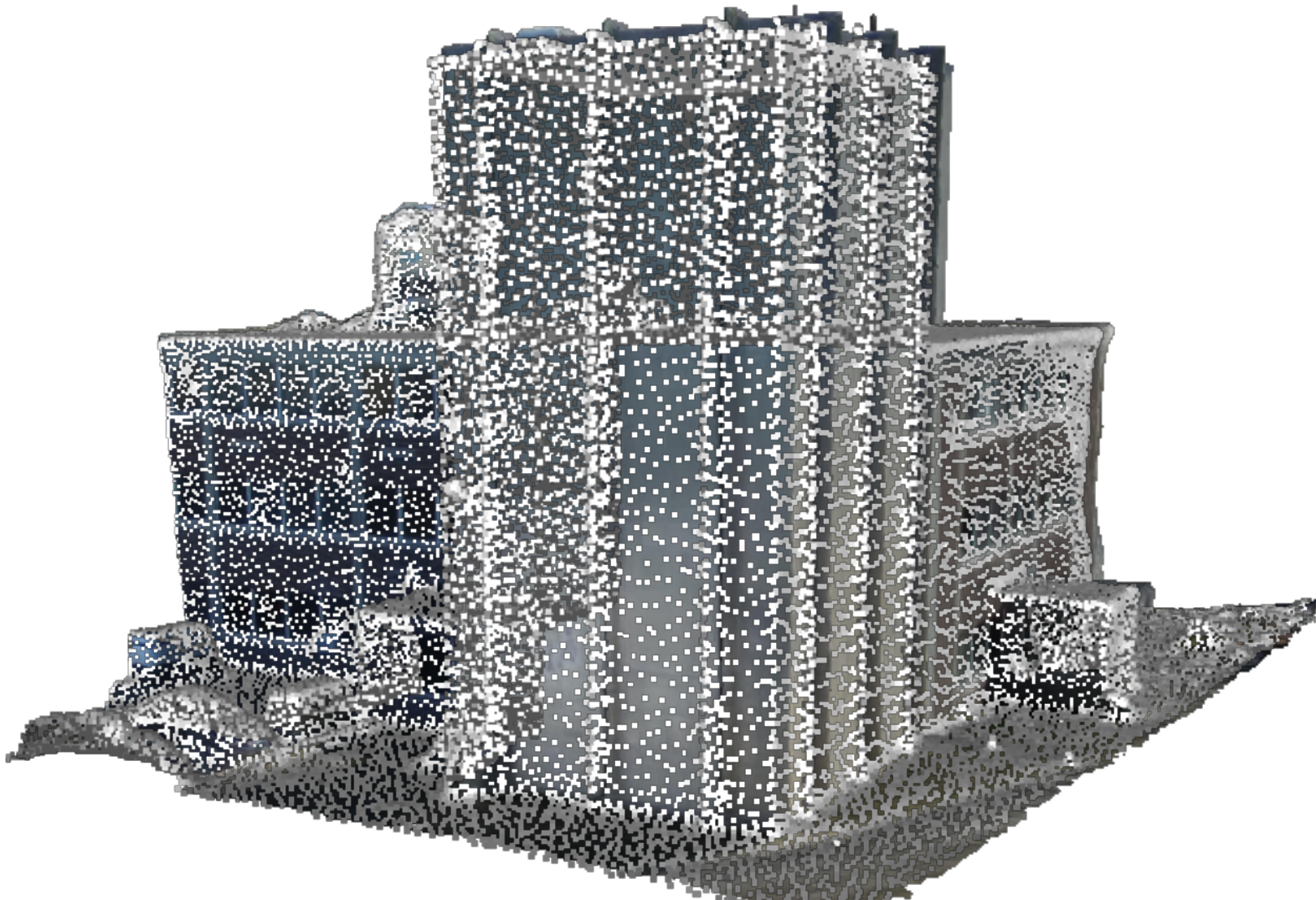
The command window at the bottom displays the following text:

```
The model database "C:\Temp\rod_detectability\re-bar0301.cae" has been opened.  
A new model database has been created.  
The model "Model-1" has been created.  
A new model database has been created.  
The model "Model-1" has been created.  
Quadratic tet elements (C3D10) will be used for the selected regions.  
Point 1: 201.96878, 35.515305, 57.761352 Point 2: 5.686744, 35.225493, 57.725507  
Distance: 196.282253 Components: -196.282036, -289.812E-03, -35.846E-03  
Global seeds have been assigned.  
Global seeds have been assigned.  
384211 elements have been generated on instance: Unif_Rebar-1
```

The bottom right corner of the software window shows the SIMULIA logo and the system tray with the date and time: 2:03 PM 4/1/2016.

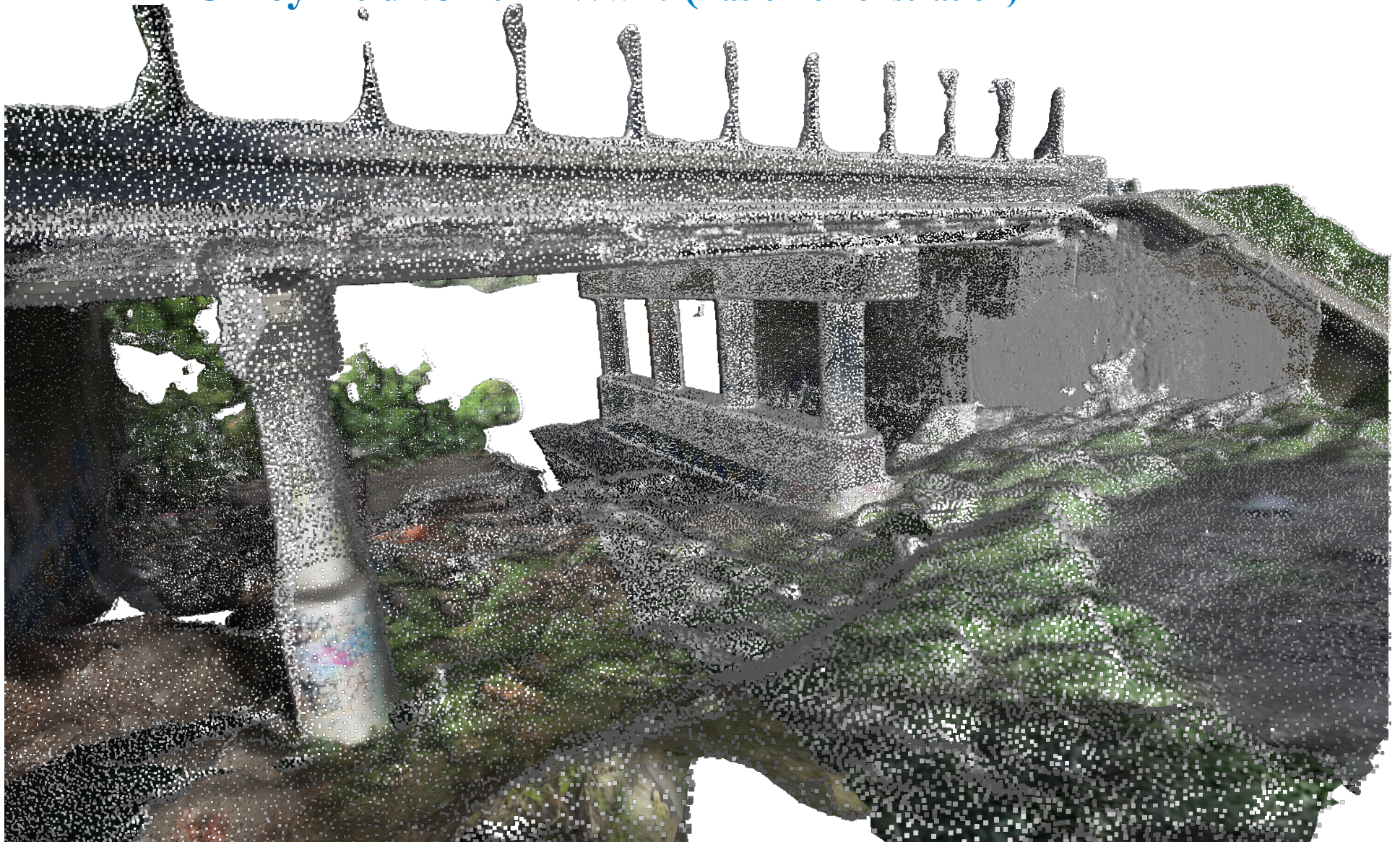
In-Situ Results (Visual Inspection)

- Pinanski Hall Umass Lowell



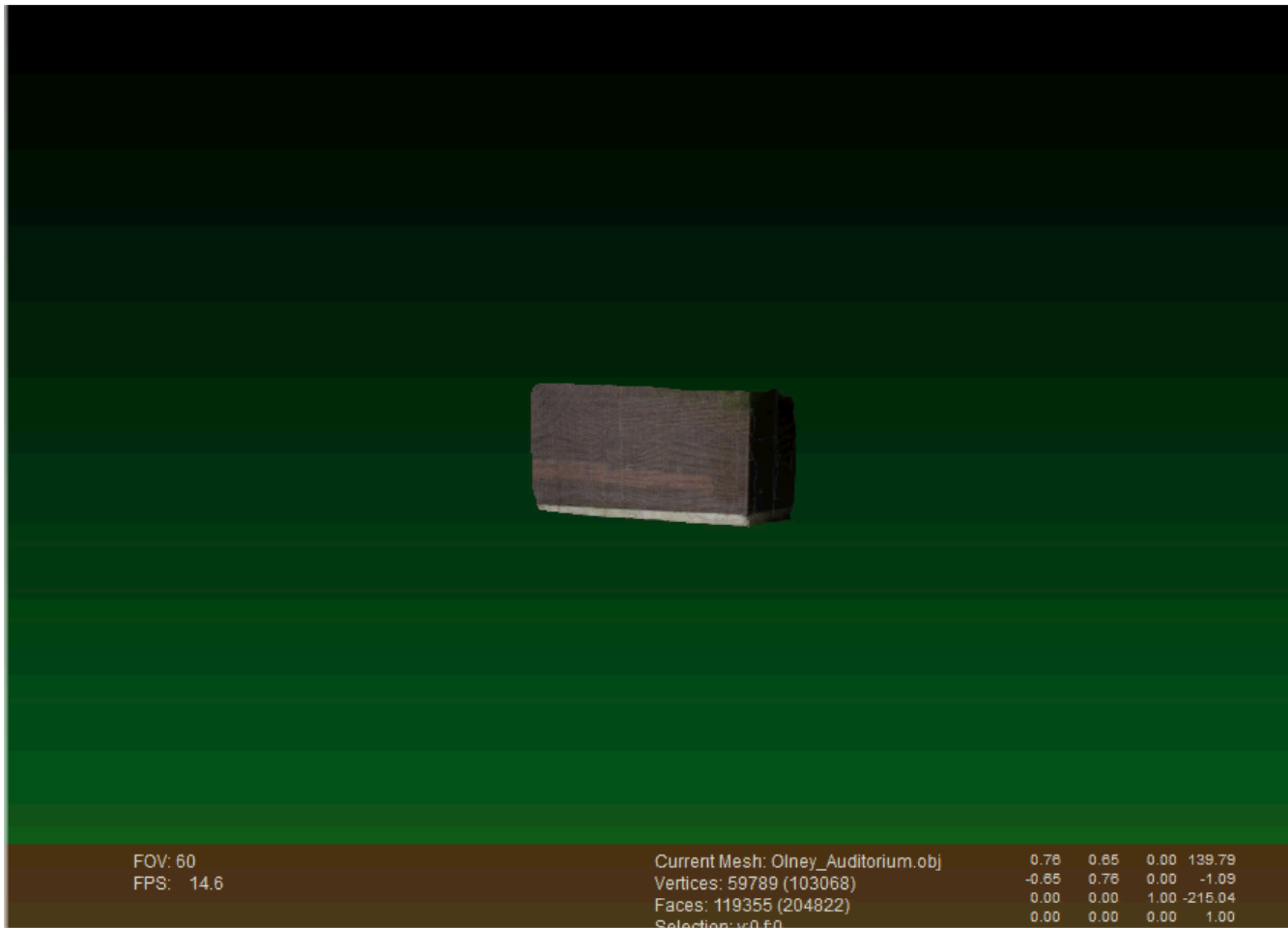
In-Situ Results (Visual Inspection)

- **Olney Auditorium Wall: (Basic Demonstration)**



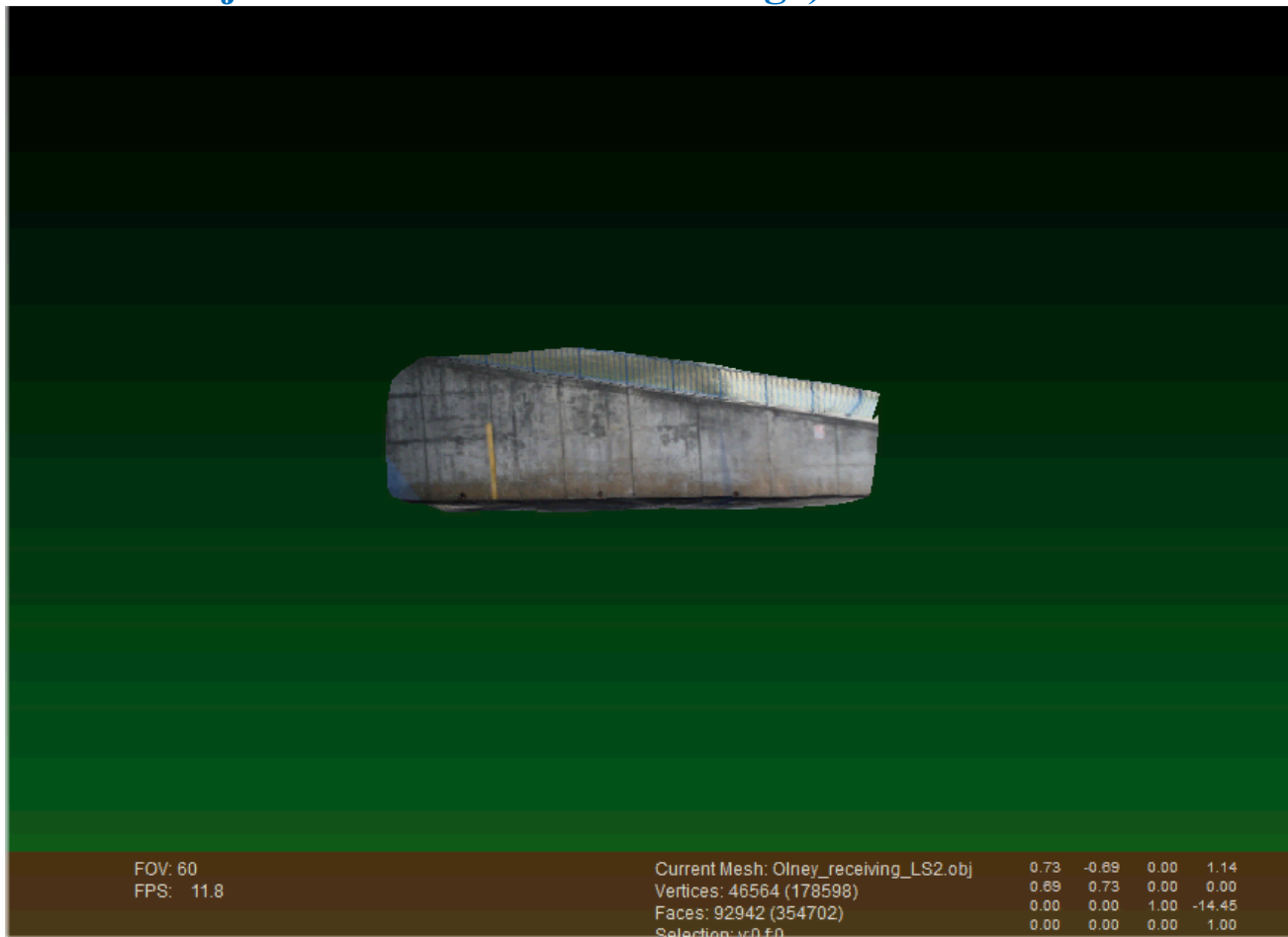
In-Situ Results (Data Registration of SAR)

- **Olney Auditorium Wall: (Basic Demonstration)**



In-Situ Results (Data Registration of SAR)

- **Loading Dock :** (shows the effect of a visible defect in conjunction with the SAR image)

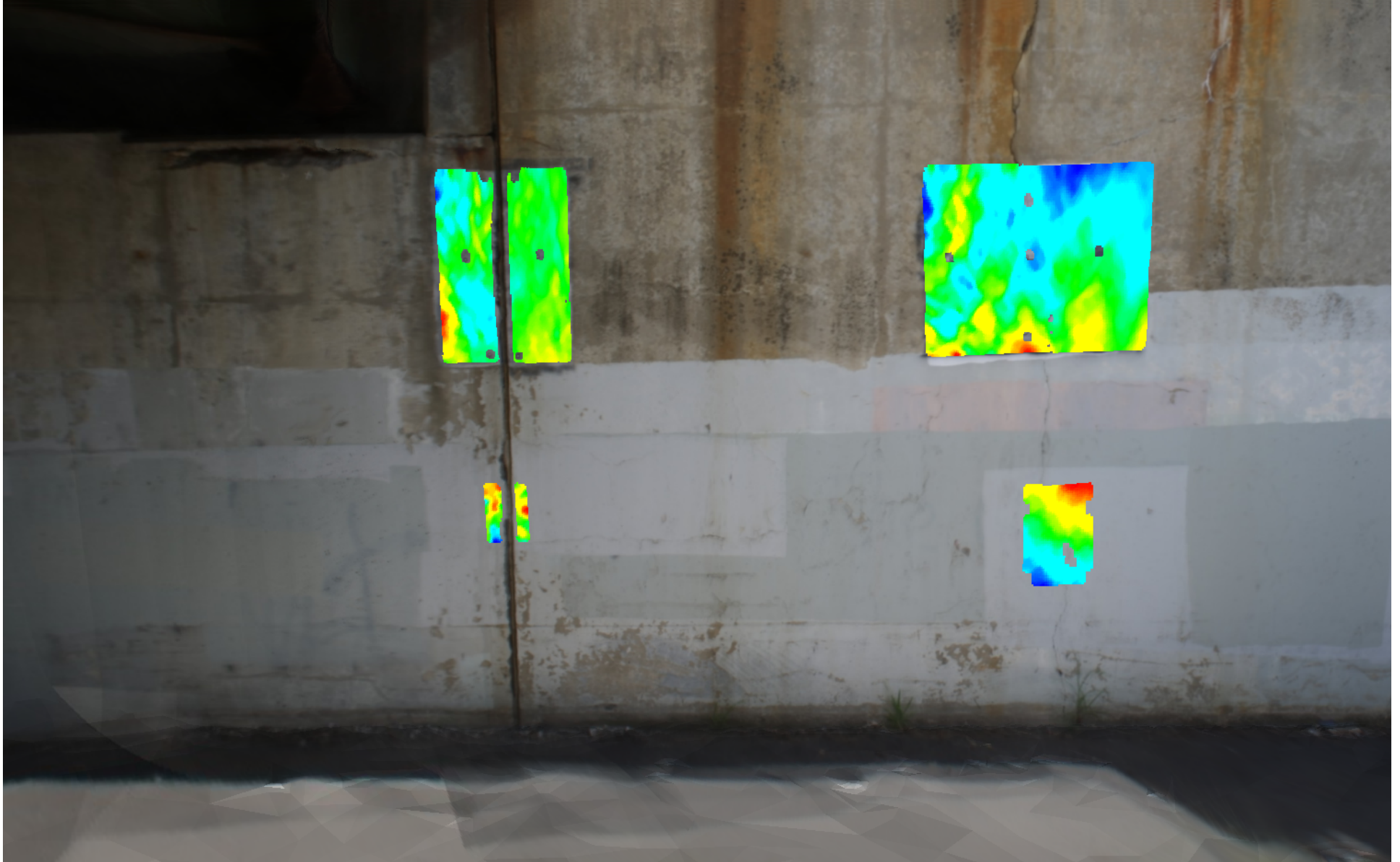


In-Situ Results (Data Registration of SAR)

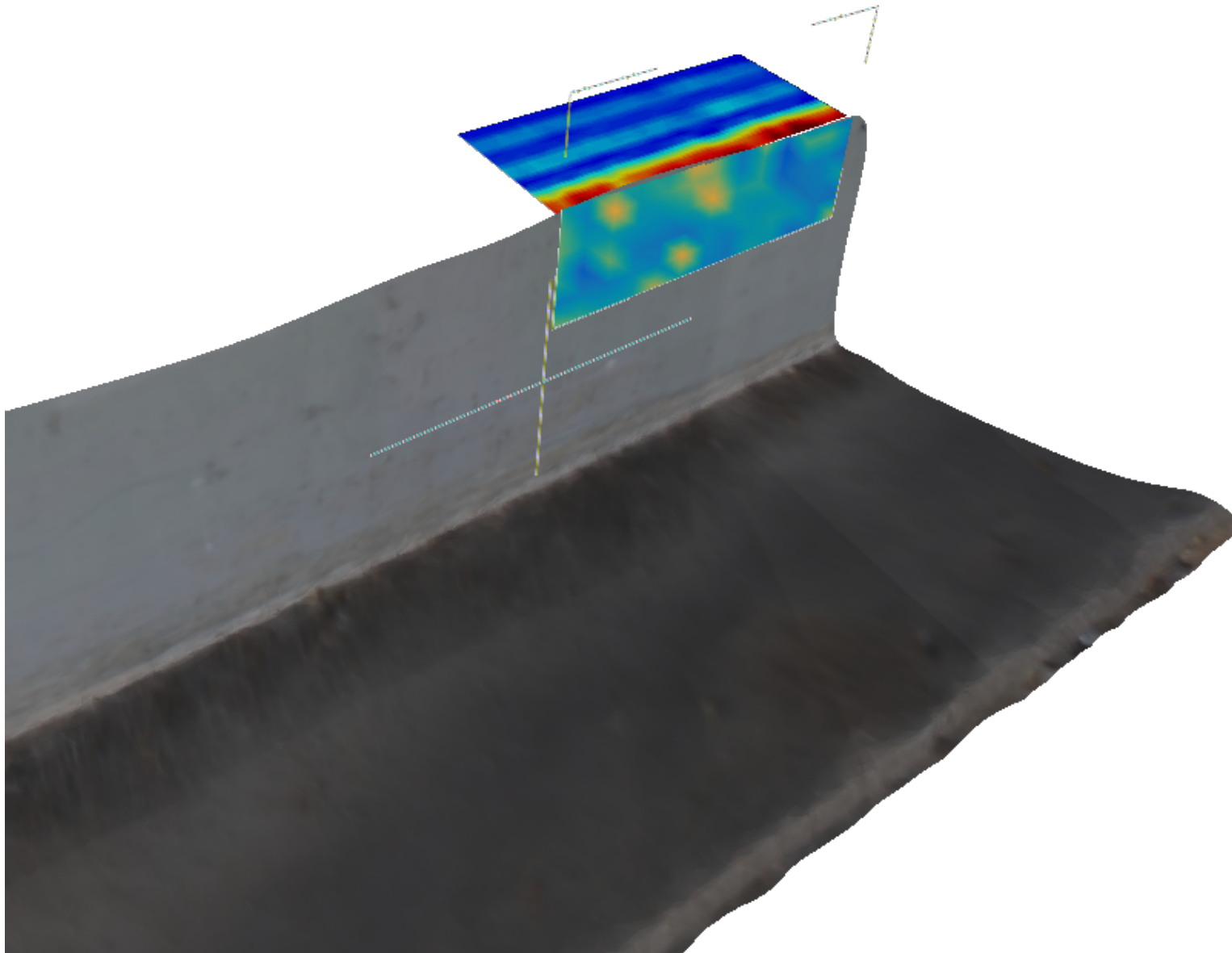
- **Pinanski:** (Demonstrates the value of positioning multiple SAR images & and how geometry effects the outcome)



In-Situ Results (Data Registration of DIC)



In-Situ Results (Data Registration of RBH)

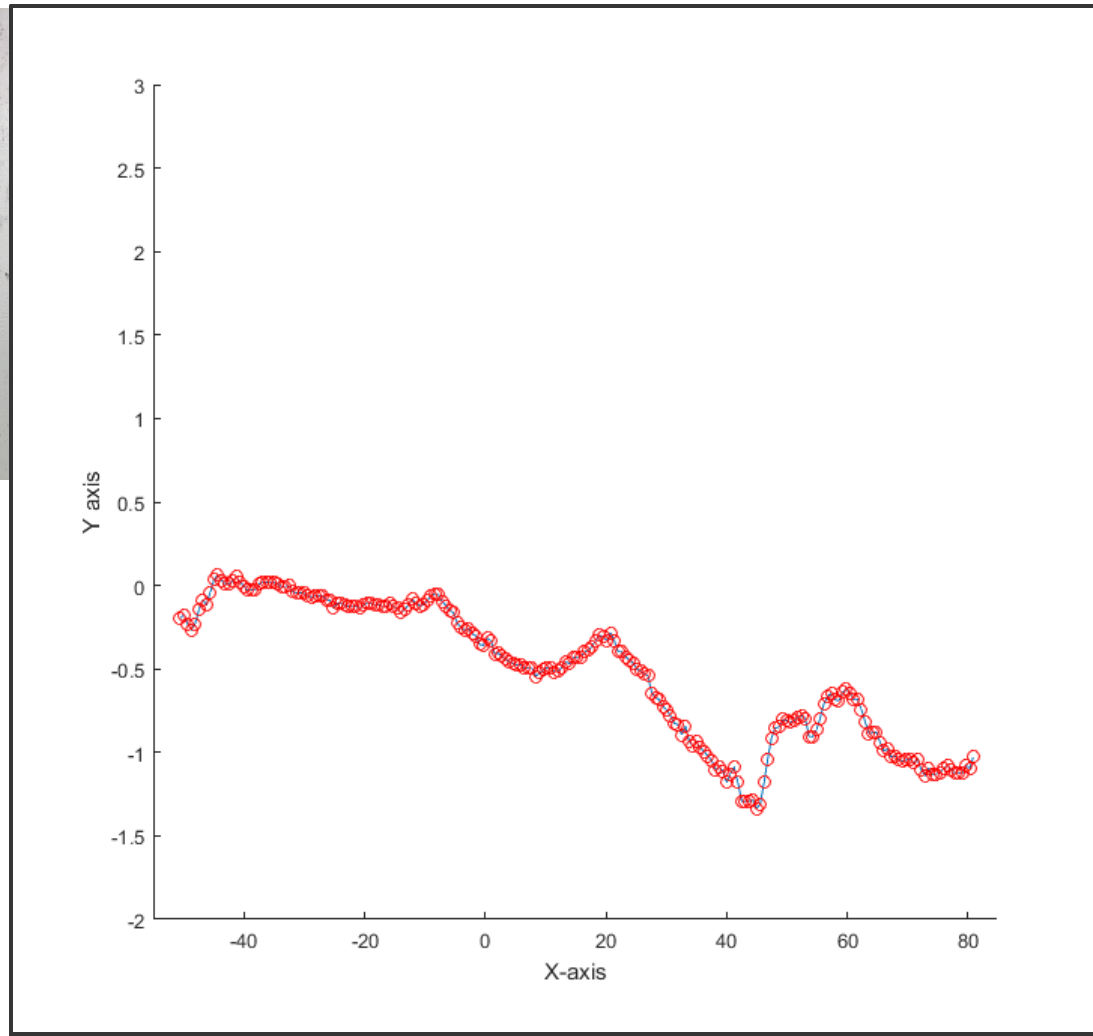


In-Situ Results (Data Registration)

- Interpolation of surface profile line (Background)



Demonstration of interpolation for $dx=.62\text{cm}$ along the cross range. At lincoln st.
Background spot scan

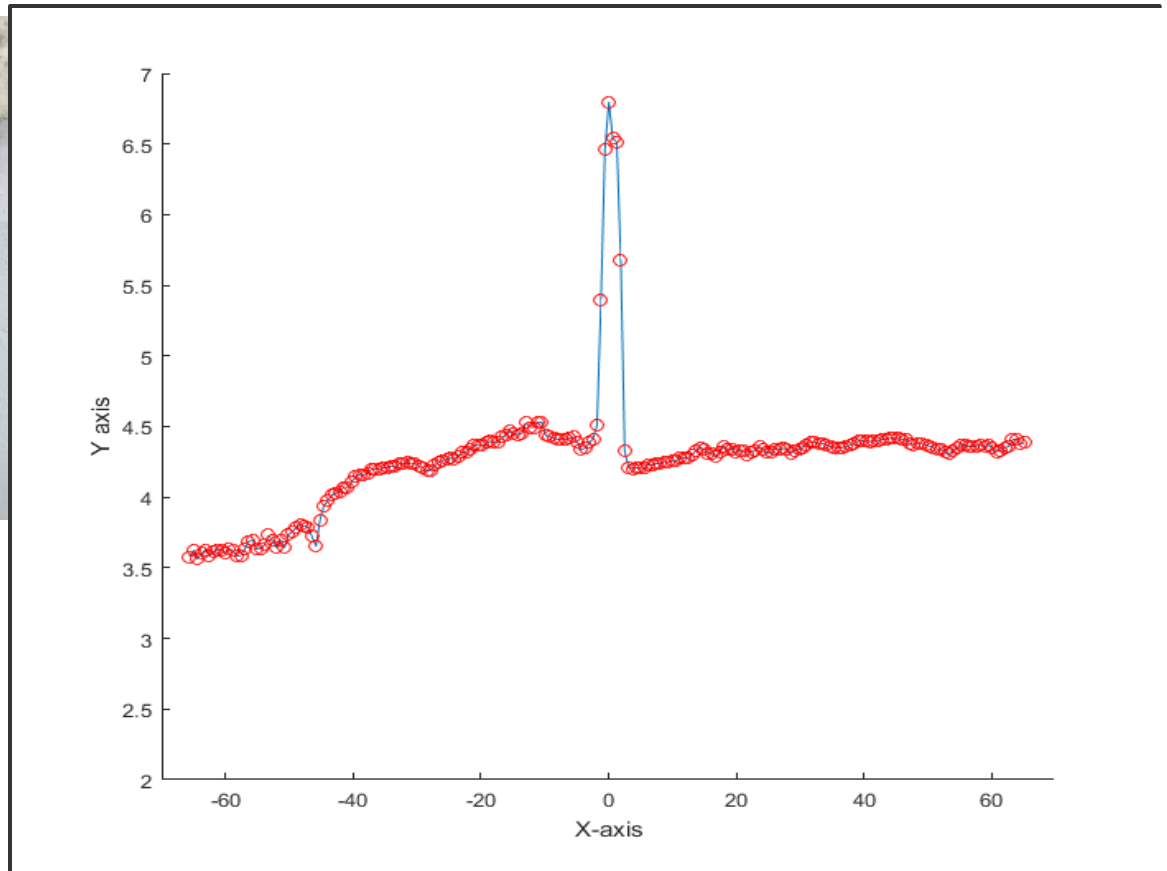


In-Situ Results (Data Registration)

- Interpolation of surface profile line Damage

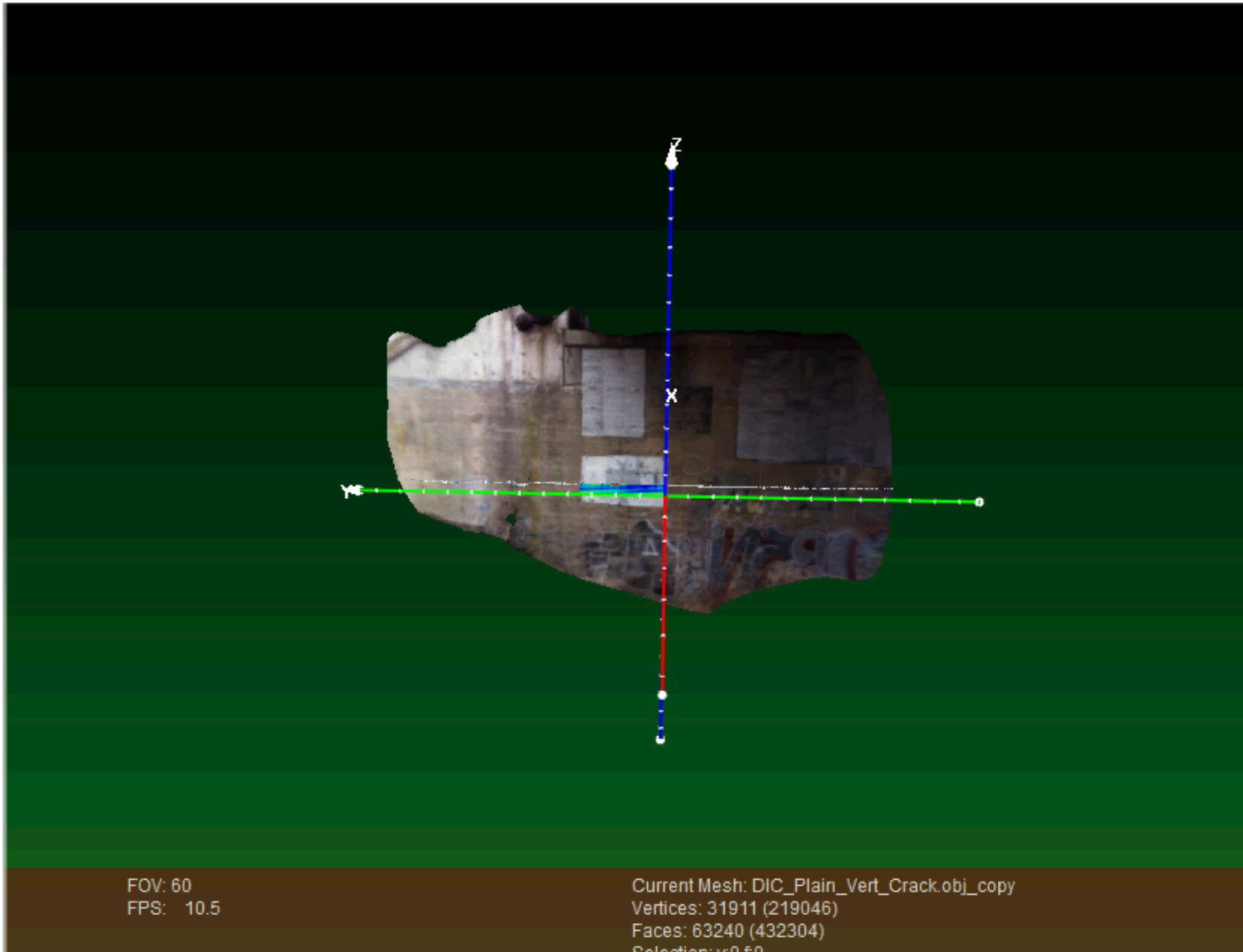


Demonstration of interpolation for $dx=.62\text{cm}$ along the cross range. At lincoln st. Damaged spot scan



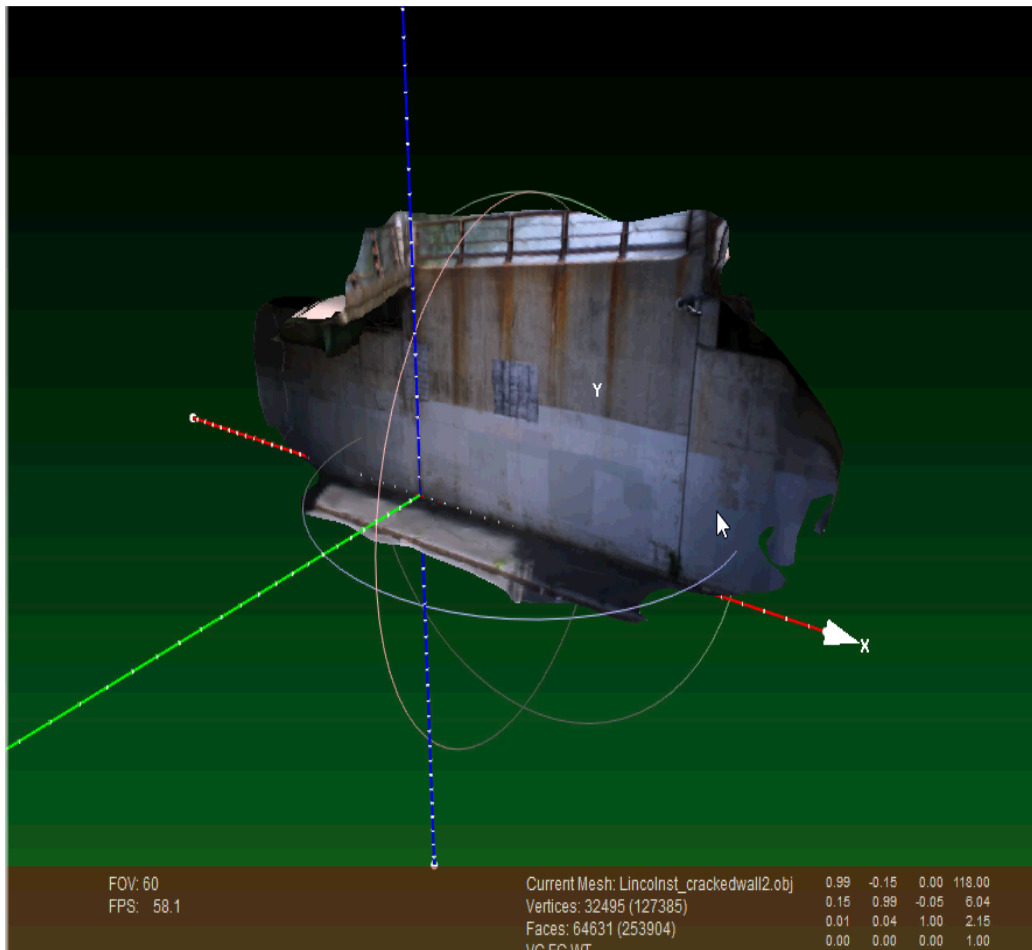
In-Situ Results (Data Registration)

- **Plain Street:** (Demonstrates the surface roughness correction)



In-Situ Results (Surface Crack Profiling)

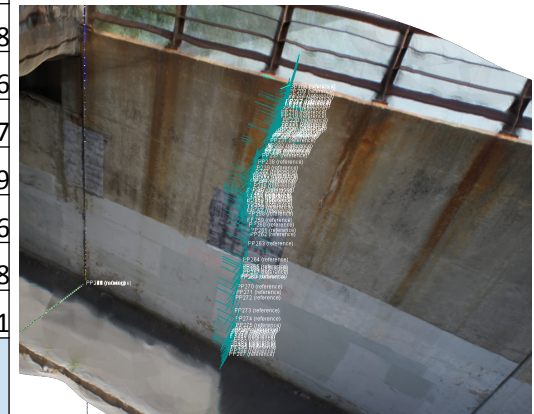
- Application: Crack length/width estimation (in-situ)



	Thickness
0	0.464119
1	0.541872
2	0.172082
3	0.503908
4	1.22098
5	0.404567
6	0.507758
7	0.29924
8	0.237928
9	0.317506
10	0.218007
11	0.769799
12	0.414236
13	0.364278
14	0.167511
Average Thickness	

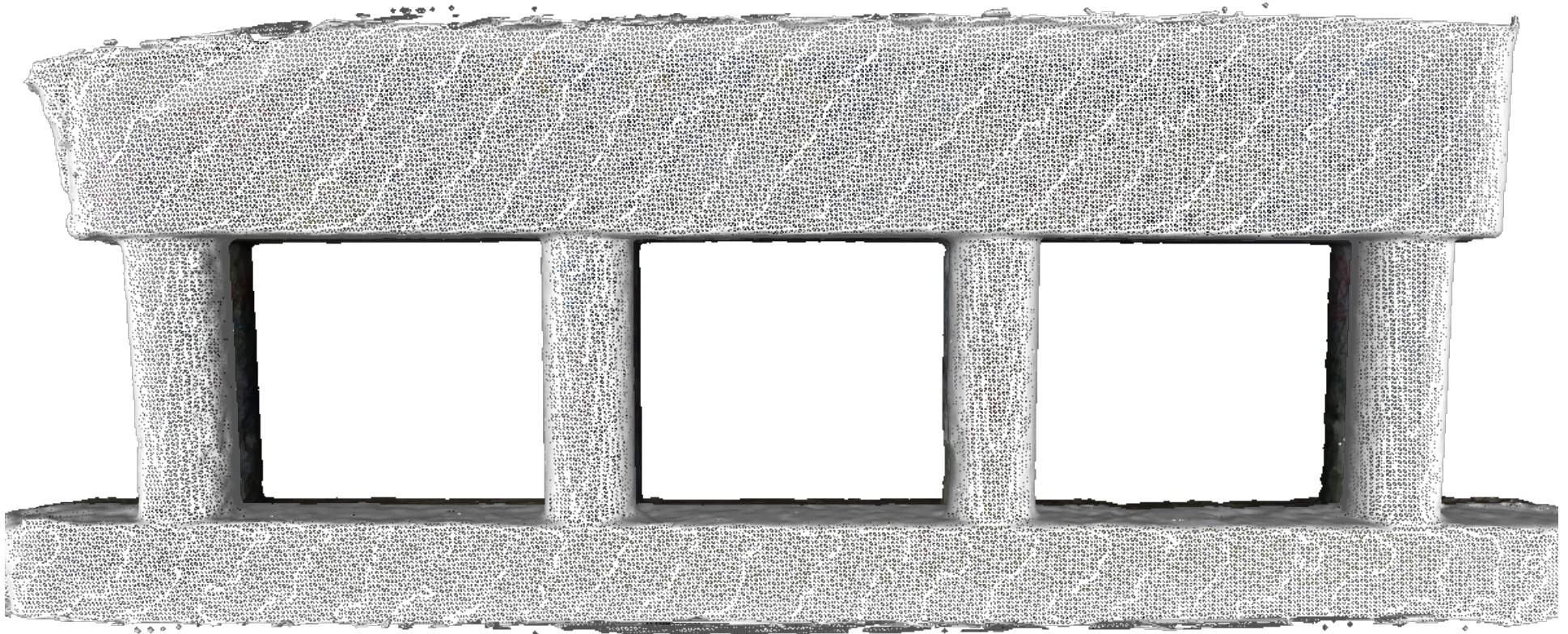
Total:	239.035in
Crack Length estimation	

Crack length calculated as the sum of the space between 81 points



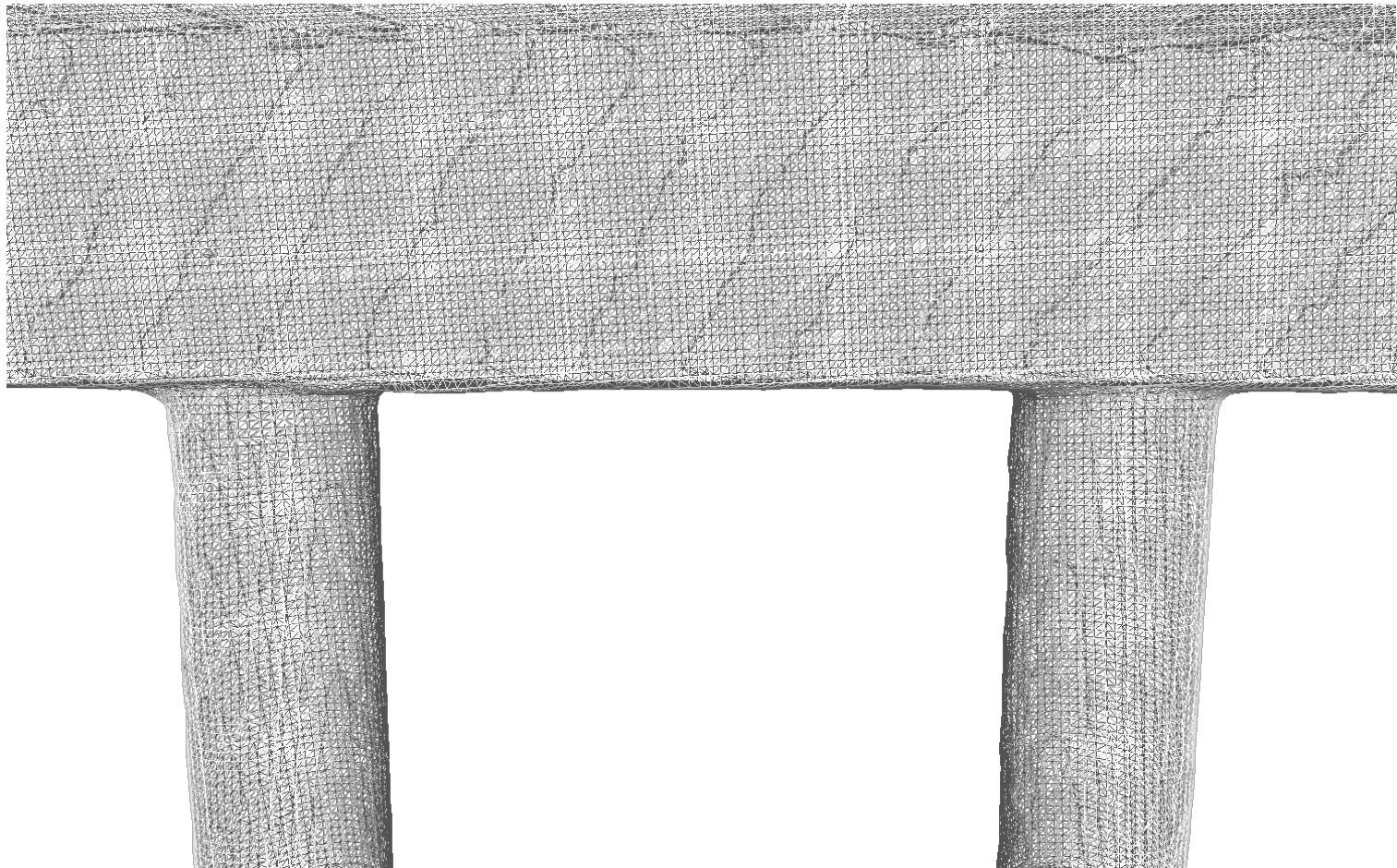
In-Situ Results (FEM)

- FEM of a column section from Plain St. bridge Lowell Ma



In-Situ Results (FEM)

- FEM of a column section from Plain St. bridge Lowell Ma



Summary and Conclusion

- **Summary of results (Lab Specimen)**
- **Geometry of photograph appropriation:** Photogrammetry relies heavily on perspective geometry to construct the 3D models.
- **Number of photographs taken:** The number of 2D photographs has a positive proportional correlation to the effectiveness or accuracy of models. Model error is reduced with an increase in photographs (n).
- **Defect location:** When multiple translations (dx, dy, dz) were considered the error would increase. This can be seen by the difference in error between PP2 (which occurred only one direction away from the origin) and PP0, with PP1 which showing a substantially higher error.
- **Geometry of the defect:** Using a flat line on a flat plane, a curved line on a curved plane, and a flat line on a curved plane, the reliability of each mode was tested. The flat line on the flat plane exhibited the least error, and the curved line on the curved plane the most.
- **Texture of the modeling surface/ apparent fiducial markers:** Because photogrammetry relies on key features to establish a projective geometry matrix, the availability of easily identifiable features is very important.

Summary and Conclusion

- **Summary of Results (Lab Specimen)**
- **Effect of number of photographs** – From our research on concrete cylinders and panels, it was found that the number of photographs (n) does not necessarily guarantee the accuracy of PCM for condition assessment. Our experimental work on laboratory specimens also suggests that, $n = 32$ photographs can be used as a lower bound for length estimation with less than a 5% average error.
- **Effect of point cloud density (PCD or p)** – A lower bound of PCD $p = 15.7194$ pts/cm³ can be used to ensure the accuracy of PCM with a 2.73% average error. An exponential function is also proposed to model this relation.
- **Surface feature of concrete specimens** –SFM PCM will be much more easily rendered for damaged structures as for intact structures, suggesting the promising potential for field applications.
- **Effect of surface curvature** – average error does not demonstrate a clear pattern with surface curvature (quantified by radius of curvature).
- **Volume estimation using PCM** – By using PCM, estimation error can be less than 5% in our results.

Summary and Conclusion

- **Summary of Results (Lab Specimen)**
- **Overall errors remained below 5%** for lengths, areas, and even volumes of concrete specimens when $PCD > 15.7194$ pts/cm³. While not entirely consistent, these results have demonstrated that photogrammetric reliability is in fact within a reasonable and acceptable range for concrete specimens (and potentially structures).
- **Comparison with ICP** – The increase in average iterative point distances in ICP models provides information correlated to the relative loading level of the specimen. The average distance differences in each loaded specimen as compared to the unloaded one can be used as an indicator to the strain (or loading) level of specimens or structures.
- **The feasibility of using PCM for surface crack profiling** is demonstrated in this research. Photogrammetric models can be used to estimate crack lengths and widths on concrete surface.
- **The increase in average iterative point distances provides data which can be correlated to the relative loading level of the specimen.** – Longitudinal and angular strain – With the use of reference markers (e.g., fiducial marker in this research), longitudinal and angular strains can be calculated from circumference data in PCM. – Radial strain – For circular targets from which photographs can be taken from all angles, radial strains can be calculated from estimated cross sectional areas in PCM.

Summary and Conclusion

- **Summary of Results (In-Situ)**
- **Photogrammetric PCM can be used for routine visual inspection**
- **Photogrammetric PCM can be used for data integration of SAR, DIC, and RBH NDE results including through interpolation of surface profiling to correct for motion of UAV platforms.**
- **Photogrammetric PCM can be used to conduct surface crack profiling, which can be used in a similar fashion to**
- **Photogrammetric PCM can be used to create geometrically accurate FEM**

Contribution

- Photogrammetry can be used to create geometrically accurate point cloud models (less than 5% error) PCM which can be used on laboratory specimens as well as in-situ structures. Furthermore, PCM can be used for visual inspection as well as data integration of Synthetic aperture radar (SAR), rebound hammer (RBH), and digital image correlation (DIC) results. Photogrammetric PCM can also be used to conduct condition assessment including geometric analysis, surface crack profiling, mechanical loading analysis and even finite element modeling (FEM).

Contribution

- The contribution of this research was the development, and calculation of error associated with analysis of concrete specimen and structures. This thesis demonstrated several original methods for surface data analysis using PCM. Additionally data acquisition, and registration techniques were developed and molded to fit the use of civil engineers both in the field and in the classroom. Laboratory methods which were researched, developed and discussed lay the ground work for material testing, as well as finite element analysis for both research and education. The work done in-situ helped to progress a best practice for NDE/I/T in a time of growing turmoil for the nations infrastructure.

Acknowledgments

Thank you to the United States Department of Transportation
for their continued support of UMass Lowell's

SEREG



References

- Matthews, N. A. 2008. *Aerial and Close-Range Photogrammetric Technology: Providing Resource Documentation, Interpretation, and Preservation*. Technical Note 428. U.S. Department of the Interior, Bureau of Land Management, National Operations Center, Denver, Colorado. 42 pp
- H. Maas and U. Hampel, “Photogrammetric Techniques in Civil Engineering Material Testing and Structure Monitoring” *Photogrammetric Engineering & Remote Sensing* Vol. 72, No. 1, January 2006, pp. 000–000.
- A. Goshtasby *2-D and 3-D Image Registration For Medical, Remote Sensing, and Industrial Applications*. John Wiley & sons, Hoboken New Jersey 2005
- E. M. Mikhail, J. S Bethel, and J.C. McGlone, *Introduction to Modern Photogrammetry*. John Wiley and Sons, Hoboken New Jersey, 2001
- Sean P. Bemis, Steven Micklethwaite, Darren Turner, Mike R. James, Sinan Akciz, Sam T. Thiele, Hasnain Ali Bangash, Ground-based and UAV-Based photogrammetry: A multi-scale, high-resolution mapping tool for structural geology and paleoseismology, *Journal of Structural Geology*, Volume 69, Part A, December 2014, Pages 163-178, ISSN 0191-8141, <http://dx.doi.org/10.1016/j.jsg.2014.10.007>.
- Tang Z, Liang J, Guo C, Wang Y; Photogrammetry-based two-dimensional digital image correlation with nonperpendicular camera alignment. *Opt. Eng.* 0001;51(2):023602-1-023602-9. doi:10.1117/1.OE.51.2.023602.
- P. Arias *, J. Armesto, H. Lorenzo, C. Ordóñez “DIGITAL PHOTOGRAMMETRY, GPR AND FINITE ELEMENTS IN HERITAGE DOCUMENTATION: GEOMETRY AND STRUCTURAL DAMAGES” ISPRS Commission V Symposium 'Image Engineering and Vision Metrology' Dep. Natural Resources Engineering and Environmental Engineering, University of Vigo, Campus Universitario As Lagoas – Marcosende s/n 36200 Vigo Spain – (parias, julia, hlorenzo, cgalan)@uvigo.es
- Aleix Cubells i Barceló “Structural assessment based on photogrammetry measurements and finite element method” Instituto Superior tecnico, Universidade de Lisboa.